Cancer Science
The official journal of the Japanese Cancer Association JCA

The side population, as a precursor of Hodgkin and Reed-Sternberg cells and a target for nuclear factor-κB inhibitors in Hodgkin's lymphoma

Makoto Nakashima,[1,2] Yumiko Ishii,[3] Mariko Watanabe,[1] Tomiteru Togano,[1] Kazuo Umezawa,[4] Masaaki Higashihara,[1] Toshiki Watanabe[2] and Ryouichi Horie[1,5]

[1]Department of Hematology, School of Medicine, Kitasato University, Minami-ku, Sagamihara; [2]Laboratory of Tumor Cell Biology, Department of Medical Genome Sciences, Graduate School of Frontier Sciences, [3]Division of Stem Cell Therapy, Center for Stem Cells and Regenerative Study, The Institute of Medical Science, University of Tokyo, Minato-ku, Tokyo; [4]Department of Applied Chemistry, Faculty of Science and Technology, Keio University, Kohoku-ku, Yokohama, Japan

(Received April 25, 2010/Revised July 19, 2010/Accepted July 22, 2010/Accepted manuscript online July 30, 2010)

Although disturbed cytokinesis of mononuclear Hodgkin (H) cells is thought to generate Reed-Sternberg (RS) cells, differentiation of Hodgkin's lymphoma (HL) cells is not fully understood. Recent studies indicate that cells found in a side population (SP) share characteristics of cancer stem cells. In this study we identified an SP in the HL cell lines, KMH2 and L428. This SP almost entirely consists of distinct small mononuclear cells, whereas the non-SP is a mixture of relatively large cells with H or RS cell-like morphology. Culture of the small mononuclear cells in the SP from KMH2 generated a non-SP. Single cell culture of the SP cells generated large cells with H or RS cell-like morphology. We found that CD30 overexpression and constitutive nuclear factor-κB (NF-κB) activity, both of which are characteristics of HL cells, are shared between the SP and non-SP cells for both KMH2 and L428. Inhibition of NF-κB induced apoptosis in both fractions, whereas the SP cells were resistant to a conventional chemotherapeutic agent doxorubicin. The results show that HL cell lines contain an SP, that is enriched for distinct small mononuclear cells and generates larger cells with H and RS cell-like morphology. The results also stress the significance of NF-κB inhibition for eradication of HL cells. (*Cancer Sci* 2010)

Hodgkin's lymphoma (HL) is a malignant lymphoma characterized by a low frequency of giant malignant cells, known as mononucleated Hodgkin (H) cells, and by multinucleated Reed-Sternberg (RS) cells in a background of reactive cells.[1] Most HL cells are B cells that originate from a germinal center B cell.[2] Previous studies using HL cell lines showed that mononuclear H cells are the precursors of multinucleated RS cells and that generation of RS cells may be associated with abortive mitosis rather than with cell fusion.[3]

CD30 is a member of the tumor necrosis factor receptor superfamily that was first identified as a cell surface molecule characteristic to H and RS cells of HL.[4] It was found that constitutively activated nuclear factor-κB (NF-κB) is a hallmark of H and RS cells and is considered to be the molecular basis of their aberrant growth and abnormal cytokine gene expression.[5] We have previously reported that overexpression of CD30 results in ligand-independent constitutive signaling that activates the transcription factors NF-κB and activator protein-1 (AP-1) in HL cells.[6,7]

Recent research indicates that most cancer cells originate from a small number of cancer cells with stem cell-like properties, called cancer stem cells (CSCs).[8] These cells are found in multiple tumor types.[9] They frequently possess MDR1 or ATP-binding cassette (ABC) transporter activities and show chemoresistance and a side population (SP) phenotype.[10] The presence of surface markers selectively expressed on CSCs are used to isolate these cells, but no marker or pattern of markers is known to prospectively identify CSCs in many tumor types. In such cases, exploitation of stem cell characteristics can be used to identify CSCs, and one such characteristic is the capacity to extrude dyes such as Hoechst 33342. Cells that exclude this dye are referred to as SP cells. These cells share characteristics of CSCs, and, specifically, they are enriched for tumor initiating capacity.[11,12]

We observed that cells present in HL cell lines and in HL patients that were previously described as ''mononuclear H cells'' are heterogeneous in their morphology. This observation led us to question if HL cells might contain SP cells. In fact, differentiation of ''mononuclear H cells'' cells was reported more than 20 years ago but was not further investigated.[13] In this study, we attempted to isolate SP cells from HL cell lines using Hoechst 33342 dye efflux as an SP marker, then we investigated the properties of these SP cells. We further discuss the significance of our findings from the viewpoint of the differentiation and the treatment of HL.

Materials and Methods

Cell culture. The HL cell lines, KMH2 and L428, were purchased from the German Collection of Microorganisms and Cell Cultures (Braunschweig, Germany). The cell lines were cultured under standard conditions in RPMI-1640 supplemented with 10% FBS.

Chemicals. Dehydroxymethylepoxyquinomicin (DHMEQ), an NF-κB inhibitor, was dissolved in DMSO.[14] Bisbenzimide H 33342 fluorochrome (Hoechst 33342) and the topoisomerase inhibitor doxorubicin were purchased from Calbiochem (Bad Soden, Germany) and Sigma-Aldrich (St. Louis, MO, USA), respectively.

Flow cytometry and SP analysis. The samples were incubated with 5 μg/mL Hoechst 33342 dye (Calbiochem) at 37°C for 60 min, with or without 30 μg/mL verapamil (Sigma-Aldrich). The cells were counterstained with 0.5 μg/mL propidium iodide (PI) (Sigma-Aldrich) to label dead cells and were analyzed with FACSAria (Becton-Dickinson, Franklin Lakes, NJ, USA) by dual-wavelength analysis using 450/20BP nm (blue) and 670/50BP nm (red) after excitation with 350-nm UV light. For sorting and culture assays of SP cells and non-SP cells, the cells were gated to exclude PI-positive cells and were sorted from the regions indicated. For phenotypic analysis, the cells were also stained with antibodies for 1 h at 4°C. When unlabeled antibodies were used, fluorescein-conjugated secondary antibody was used. Finally, the cells were washed and resuspended in PBS

[5]To whom correspondence should be addressed.
E-mail: rhorie@med.kitasato-u.ac.jp

doi: 10.1111/j.1349-7006.2010.01693.x

containing 2% FBS and PI, then analyzed by FACSAria (Becton-Dickinson) using the FlowJo analysis program (Tree Star, Ashland, OR, USA).

Antibodies used were obtained from the following companies. CD19, CD34, CD44, CD133, and CD20 (all from Becton-Dickinson), CD30 (Dako, Kyoto, Japan), CD40 (Beckman Coulter, Brea, CA, USA), CD15 (EXBIO Praha, Vestec, Czech Republic), CD117, HLA-DR (Cell Signaling Technology, Danvers, MA, USA). Isotype matched control antibody was obtained from Becton-Dickinson.

Immunohistochemistry. Fluorescence immunostaining was carried out on cultured cells as previously described.[15] Primary antibodies used were: anti-Ki-67 (DAKO), anti-JunB (C-11), anti-Bcl-xL (H-62), anti-cellular FLICE-like inhibitory protein (c-FLIP) (H-202; Santa Cruz Biotechnology, Santa Cruz, CA, USA), and anti-activated NF-κB p65 (Chemicon International, Temecula, CA, USA). Signals were detected using a fluorescence microscope (BX50F; Olympus, Tokyo, Japan).

Immunostaining of CD30 on paraffin-embedded specimens of primary HL samples with informed consent was carried out as previously described.[7]

Analysis of cell viability and apoptosis. Cell viability was analyzed using a Trypan blue dye exclusion test as described.[16] The experiment was carried out in triplicate, and at least 100

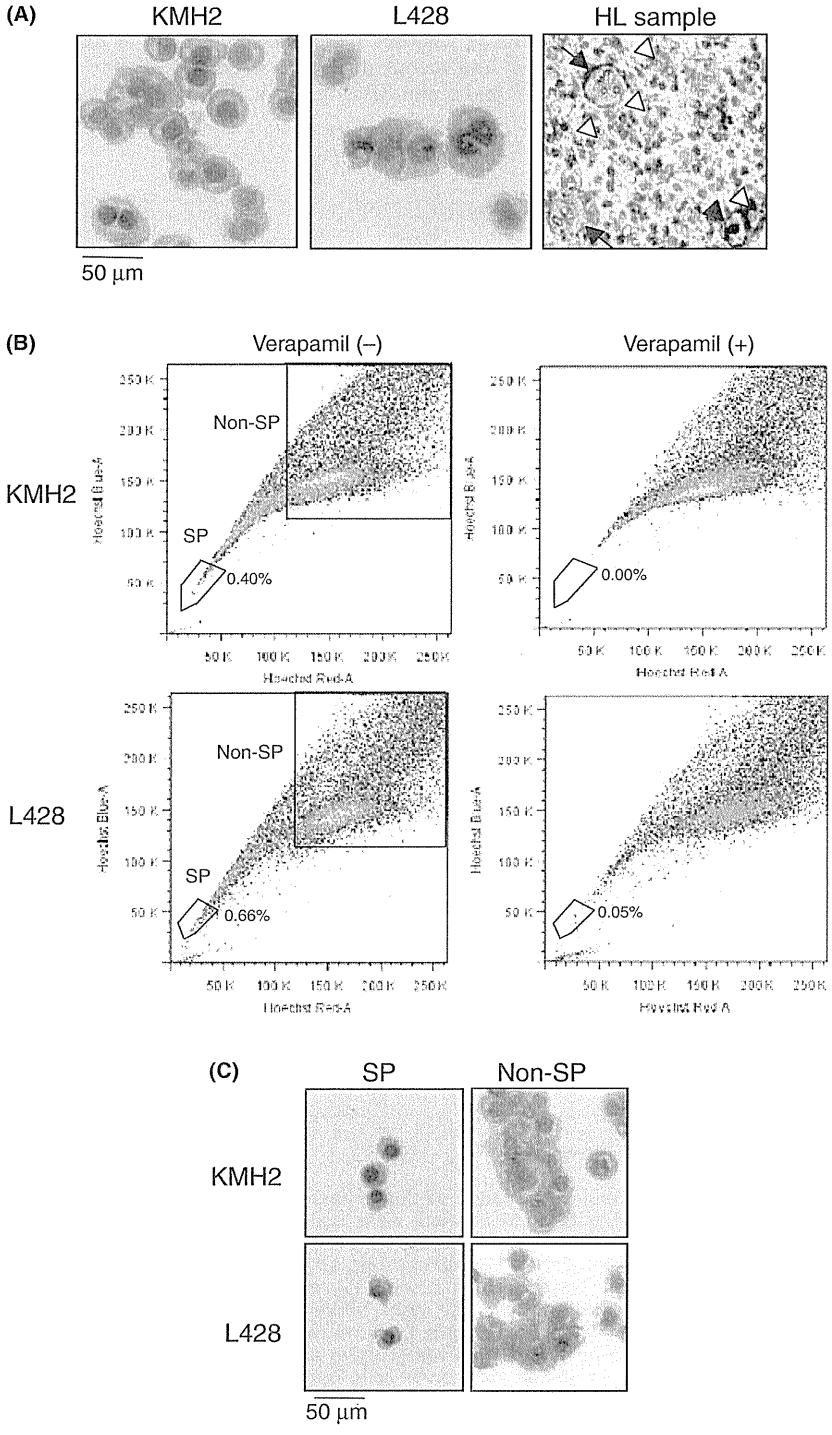

Fig. 1. Morphological appearance of mononuclear Hodgkin's lymphoma (HL) cells and side population (SP) analysis of HL cell lines KMH2 and L428. (A) The HL cell lines were stained with Giemsa (left and middle panels). Hodgkin's lymphoma cells in primary HL samples (n = 5) were detected by anti-CD30 antibody and a representative result is shown (right panel). The black arrows and arrowhead indicate Reed-Sternberg cells and a Hodgkin cell, respectively. The white arrowheads indicate smaller HL cells. (B) Analysis of SP cells in HL cell lines. The SP fractions of both cell lines were reduced by treatment with verapamil. The percentage of SP cells is indicated in each graph. (C) Morphology of SP and non-SP cells, both stained with Giemsa.

doi: 10.1111/j.1349-7006.2010.01693.x

cells per experiment were counted. To quantify apoptosis, cells were stained using an annexin V–Azami-Green apoptosis detection kit (MBL, Nagoya, Japan). The cells were photographed through a UV filter on a fluorescence microscope.

Statistical analysis. Differences between mean values were assessed using a two-tailed *t*-test. A *P*-value of <0.05 was considered to be statistically significant.

Results

Identification of an SP consisting of distinct small mononuclear cells in HL cell lines. Large mononuclear cells observed in HL are usually called H cells. However, mononuclear cells of the HL cell lines consist of cells showing heterogeneous morphology (Fig. 1A, left and middle). Hodgkin's lymphoma cells can be identified by overexpression of CD30. We identified CD30-overexpressing smaller mononuclear cells among multinucleated RS cells and large mononucleated H cells in lymph nodes of HL patients (a representative photograph is shown in the right panel of Fig. 1A). Control experiments using isotype-matched primary antibody showed negative staining (data not shown). These observations led us to hypothesize the existence of precursor cells from which neoplastic component characteristics for HL, that is, H and RS cells, might be derived. Based on these observations, we carried out SP analysis of the HL cell lines and identified a minor population of SP cells (Fig. 1B). These SPs were enriched for small mononuclear cells with distinct morphology, whereas the non-SPs consisted of larger heterogeneous cells, which included cells with H or RS cell-like morphology (Fig. 1C).

Side population cells generate cells with H or RS cell-like morphology. We next separated the SP from KMH2 and determined if cells with H or RS cell-like morphology could be derived from this SP fraction. Culture of the SP for 14 days generated a non-SP and reconstituted the original cell line pattern with both an SP and a non-SP (Fig. 2A). The morphology of the

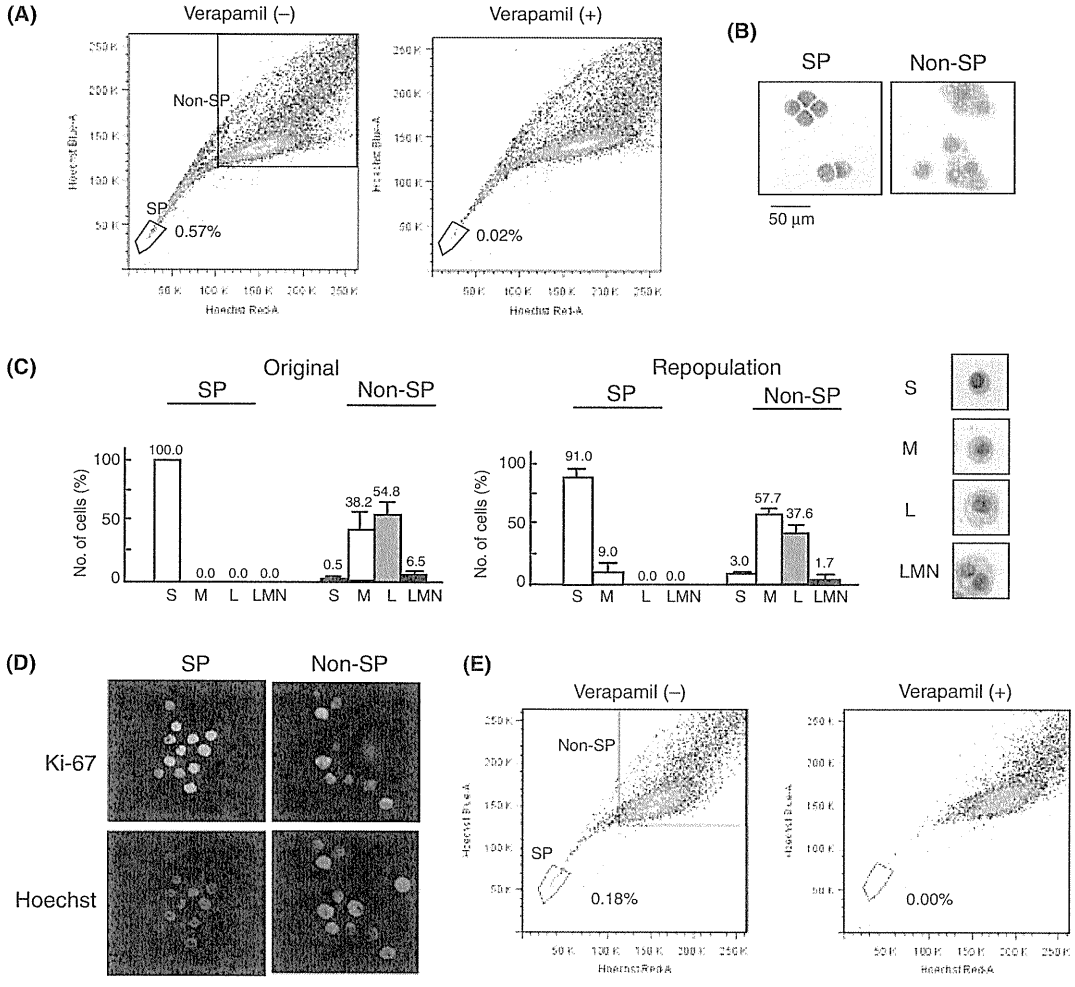

Fig. 2. Side population (SP) analyses of cultured SP and non-SP cells. (A) Side population analysis of the SP fraction cultured for 14 days. The SP fraction of KMH2 cells (5×10^3) was cultured for 14 days, then the presence of SP and non-SP fractions were analyzed. (B) Morphology of SP and non-SP cells derived from the SP fraction cultured for 14 days. Both SP and non-SP cells were stained with Giemsa. (C) Morphology of SP and non-SP cells in the original KMH2 cells (Original) and those derived from 2×10^3 cells of the SP fraction cultured for 14 days (Repopulation). The absolute number of the cells in the repopulation was 8×10^6. The morphology was classified as small (S), medium (M), large (L), or large multinucleated (LMN). Representative morphologies of each classification are indicated on the right. More than one hundred cells were classified for each fraction at least three times and representative results are presented as bar graphs. Data are the means ± SD. The mean values are indicated above each bar graph. (D) Ki-67 staining of SP and non-SP cells from the original KMH2 using an anti-Ki-67 antibody. The cells were counterstained with Hoechst 33342. Detection of Hoechst was varied between the SP and non-SP cells, because of the very weak signal in the SP cells. (E) Side population analysis of the non-SP fraction cultured for 14 days. The non-SP fraction of KMH2 cells (5×10^3) was cultured for 14 days, then the presence of SP and non-SP fractions were analyzed.

SP and non-SP cells was very similar to that observed in Figure 1(C) (Fig. 2B). To clarify the cell morphology in these populations, we morphologically classified and counted SP and non-SP cells of the original and the reconstituted samples. The results indicate that the original SP almost entirely consists of typical small mononuclear cells, and the repopulated non-SP contains abundant large cells and a small fraction of large multinucleated cells. The repopulation of SP cells was accompanied with the increase in cell number, suggesting that the proliferation and differentiation of SP cells occurred during repopulation (Fig. 2C).

We examined whether SP cells were replicating as actively as non-SP cells by anti-Ki-67 antibody. Ki-67 reacts with nuclei of cells in G_1, S, and G_2 and mitosis but not with G_0 cells, and has been shown to be generally positive in H and RS cells.[3] Ki-67 was more strongly expressed in SP cells than in non-SP cells. In addition, the SP cells showed almost all Ki-67 positive, whereas a part of the non-SP cells were negative, indicating that SP cells are more actively replicating than non-SP cells (Fig. 2D). Control experiments showed negative staining (data not shown). Collectively, these results support the notion that small mononuclear cells found in the SP are actively replicating and generate cells with H or RS cell-like morphology.

However, non-SP cells also reconstituted the original cell line pattern with both an SP and a non-SP (Fig. 2E). This result appears to conflict with the result of reconstitution by SP cells, however, the reconstitution by non-SP cells has already been reported by several published works, supporting the notion that CSC-like precursor cells are partly, but not exclusively, enriched in an SP.[17,18] The SP has been hypothesized to be linked by a very small population of cells in the non-SP, although contamination of a small amount of SP cells in the non-SP cannot be ruled out.[19]

Single SP cell generates larger mononuclear cells and large multinucleated cells. To confirm the notion that the small mononuclear cells in the SP generate cells with H or RS cell-like morphology, single cell analysis was carried out. The results of single cell culture for 7 days showed that both fractions could proliferate, although the SP cells were prone to form mulberry-formed colonies (Fig. 3A). However, polynucleated cells failed to proliferate, as reported previously.[13] The SP cells generated larger cells, whereas the non-SP cells proliferated as large cells (Fig. 3B,C). This indicates that the small mononuclear cells in the SP are a major pool for generation of large cells in the non-SP. These results further support the notion that the small cells found in the SP generate cells with H or RS cell-like morphology.

Side population cells share biological characteristics of HL with non-SP cells. To compare the phenotype of SP and non-SP cells, we carried out extensive cell marker analysis. We focused on markers related to stem cells,[20] HL,[1] and B cells. The results indicate that the expression pattern of both markers is very similar between the SP and non-SP cells (Fig. 4A). Overlaid histograms of each marker are shown in Figure S1. Although it was not possible to show markers that discriminate between the SP and non-SP cells, the conservation of HL markers, especially the same level of expression of CD30 in both fractions, indicates that the biological basis previously reported in HL may be also applicable to the SP cells.

Analysis of CD30 expression in SPs and non-SPs of KMH2 and L428, using FACS, showed a very similar CD30 mean fluorescence intensity and histogram, suggesting that CD30 is also overexpressed in SP cells (Fig. 4B). We also determined the level of activation of NF-κB and AP-1 using immunofluorescence. The results showed the same pattern of expression of activated RelA and JunB in both fractions[7,15] (Fig. 4C). Control experiments showed negative staining (data not shown). These results indicate that the biological bases characteristic for HL appear to be shared between the SP and non-SP cells.

Side population cells are resistant to doxorubicin, but are sensitive to NF-κB inhibition. We and others have reported that constitutive NF-κB activation is a molecular target of HL cells.[5] However, it is entirely unknown how effective NF-κB inhibition is against the SP of HL. Therefore, we determined the effect of NF-κB inhibition on the viability and apoptosis of the SP cells using the NF-κB inhibitor DHMEQ.[21] Treatment with DHMEQ effectively abrogated constitutive NF-κB activation by inhibiting nuclear localization of activated RelA (Fig. 5A). Treatment with DHMEQ reduced the viable cell number of both fractions, suggesting DHMEQ induced the death of these cells (Fig. 5B). In contrast, treatment with doxorubicin, a key conventional chemotherapeutic agent for HL, potently reduced the viable cell number of the non-SP, but not the SP cells (Fig. 5B). Both the non-SP and SP cells treated with DHMEQ stained positive for annexin V (Fig. 5C). These results show that the reduction in viability of the SP cells with DHMEQ is accompanied by apoptosis and indicate that inhibition of NF-κB may be effective for eradication of HL cells by inducing apoptosis in their precursor cells, which appear to be resistant to conventional chemotherapeutic agents.

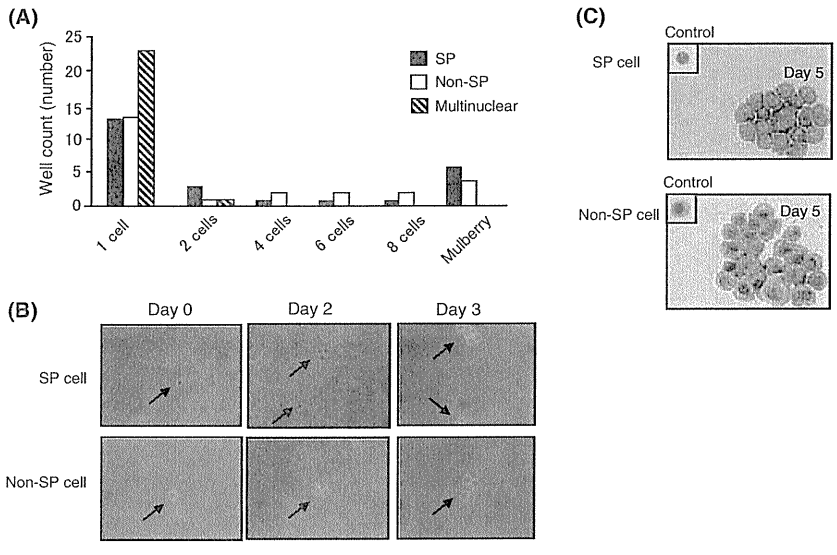

Fig. 3. Single cell culture of side population (SP) cells. Twenty-four cells sorted by FACSAria in each fraction were served for single cell culture in 96-well plates for 7 days and their proliferation was analyzed by microscopic observation. Data represent three independent experiments. (A) The number of cells in each well was counted at 7 days, and the results are shown as bar graphs. (B) Microphotographs of representative proliferation of a single cell at the indicated time points. Cells are indicated by arrows. (C) The SP or non-SP cells harvested from a single well at day 5 were cytospined and stained with Giemsa. Representative cases are shown. Side population and non-SP cells at day 0 were stained and a representative cell for each fraction, although not identical to the original cell of the harvested cells, is shown as an inset and served as control presentation.

doi: 10.1111/j.1349-7006.2010.01693.x

(A)

KMH2		SP positive (%)	Non-SP positive (%)
Stem cell-related marker	CD34	0.00	0.01
	CD44	98.88	99.25
	CD117	0.00	0.00
	CD133	2.98	1.77
	HLA-DR	73.20	65.08
Hodgkin-related marker	CD30	100.00	99.70
	CD40	100.00	100.00
	CD15	99.70	97.07
B cell-related marker	CD19	0.00	0.00
	CD20	0.00	0.00

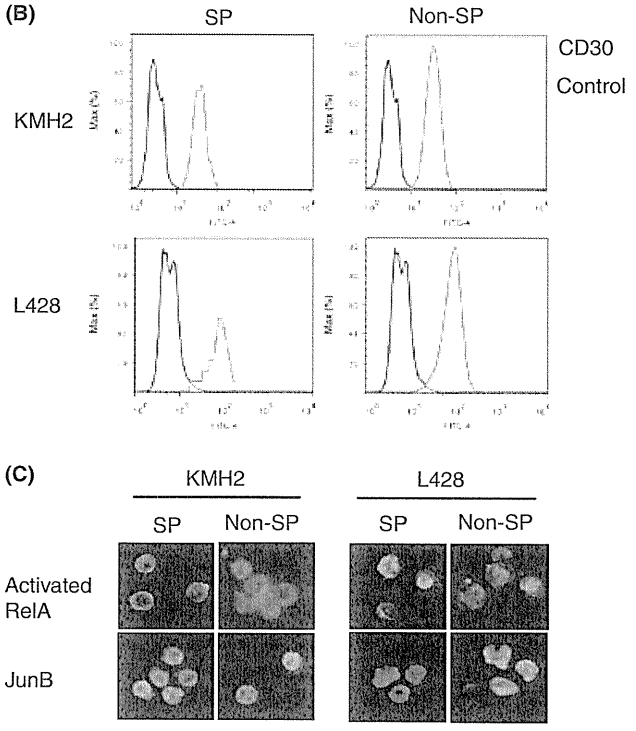

Fig. 4. Expression of key Hodgkin's lymphoma cell molecules in side population (SP) and non-SP cells. (A) Summary of the phenotype. The positive percentage for each marker is shown. (B) CD30 expression analyzed by FACS analysis. Stain of the total population by isotype-matched antibody served as control. (C) Activation of nuclear factor-κB (RelA) and activator protein-1 (JunB). Cells were immunostained with anti-activated RelA or anti-JunB as described.

Previous reports indicated frequent expression of anti-apoptotic molecules Bcl-xL and c-FLIP and involvement of their activity in the survival of HL cells.[22,23] We previously showed the downregulation of Bcl-xL and c-FLIP upon blocking of NF-κB activity and indicated the involvement of these molecules in the survival of HL cells dependent on NF-κB signaling.[15] Based on these backgrounds, we examined the effect of an NF-κB inhibitor DHMEQ on SP and non-SP cells of HL cell line, KMH2. The results clearly showed the downregulation of Bcl-xL and c-FLIP by treatment with DHMEQ in both SP and non-SP cells, indicating Bcl-xL and c-FLIP are potential key molecules, which support the survival of not only non-SP cells, but also SP cells (Fig. 5D).

To obtain an insight into the mechanism of doxorubicin resistance of SP cells of HL cell lines, the SP and non-SP cells were treated under the same conditions as shown in Figure 5(B). The cells were cultured with doxorubicin for 1 h then the cellular doxorubicin distribution was analyzed. The results showed that both cellular fractions incorporated doxorubicin (Fig. 5E).

Discussion

We have identified SPs in HL cell lines. These SPs are enriched for small mononuclear cells with distinct morphology, whereas the non-SPs consist of larger heterogeneous cells, which include cells with characteristic H or RS cell-like morphology. Culture of SP cells of KMH2 reconstituted the original cell line pattern with both an SP and a non-SP. As the isolated SP cells were highly pure and almost entirely consisted of typical small mononuclear cells, the small mononuclear cells were thought to be responsible for the reconstitution. This is further supported by the result that the single cell analysis of the cells sorted from the SP generates larger heterogeneous cells. The SP cells showed strongly positive for proliferation marker Ki-67 compared with the non-SP cells. Previous reports that stated that SP cells retain high proliferation property support this notion.[24,25] SP cells have been reported to share characteristics of CSCs, in particular, SPs are enriched for tumor initiating capacity[12]. Generally CSCs are considered to be resistant to conventional chemotherapeutic agents. The SPs identified in HL cell lines showed resistance to a conventional agent, doxorubicin, compared with the non-SPs, indicating the SPs appear to share important CSC-like properties. These results indicate the possibility that the SP cells identified here may represent "precursor cells" of the characteristic neoplastic H and RS cells of HL.

A previous report hypothesized that a very small population of slow cycling CSC-like cells without ABCA2 expression exist in a non-SP. After acquisition of ABCA2 expression, these cells, which are identified as SP cells, have been thought to act as fast cycling tumor progenitors.[19] Culture of the non-SP of KMH2 cells for 14 days also reconstituted the SP and non-SP pattern, indicating the possibility that the small mononuclear cells found in the SP of HL cell lines represent the fast cycling tumor progenitors. The single cell culture of the non-SP cells generally did not generate small mononuclear cells. Therefore, we prefer the notion that a very small fraction of non-SP cells, which share their morphology with SP cells, are candidates for slow cycling CSC-like cells. In fact, we found small mononuclear cells in the non-SP of KMH2 (Fig. 2C). However, we could not characterize these cells in this study, because no pattern of markers is known to prospectively identify these cells.

A previous study indicated the existence of clonogenic H cells in L428 and the relationship of the continuum of malignant mononuclear H and multinuclear RS cells. This study showed that single cloned mononuclear H cells were clonogenic and H and RS cells arose in a 10% cloning efficiency, whereas small abortive colonies sometimes arose from RS cells. This study was reported more than 20 years ago but was not further investigated.[13] The result appears to indicate that H cells retain proliferative potential and generate RS cells, although the morphology of those clonogenic mononuclear cells was not described in detail. Our results provide a new insight to the above study and indicate the existence of a very small population of "precursor cells" with distinct morphology and the SP phenotype among mononuclear cells of HL cell lines. A recent report indicated that aldehyde dehydrogenase $(ALDH)^+$ $CD20^+$ $CD30^-$ $Ig\lambda^+$ clonotypic B cells exist in the blood of HL patients and that these cells in the KMH2 and L428 cell lines can function as precursor cells for H and RS cells,[26] however, this notion is currently controversial.[27] The SP cells that we identified in HL cell lines do not represent the above described cell fraction, because they are $CD20^-$ $CD30^+$. $ALDH^+$ $CD20^+$ $CD30^-$ $Ig\lambda^+$ clonotypic B cells were isolated

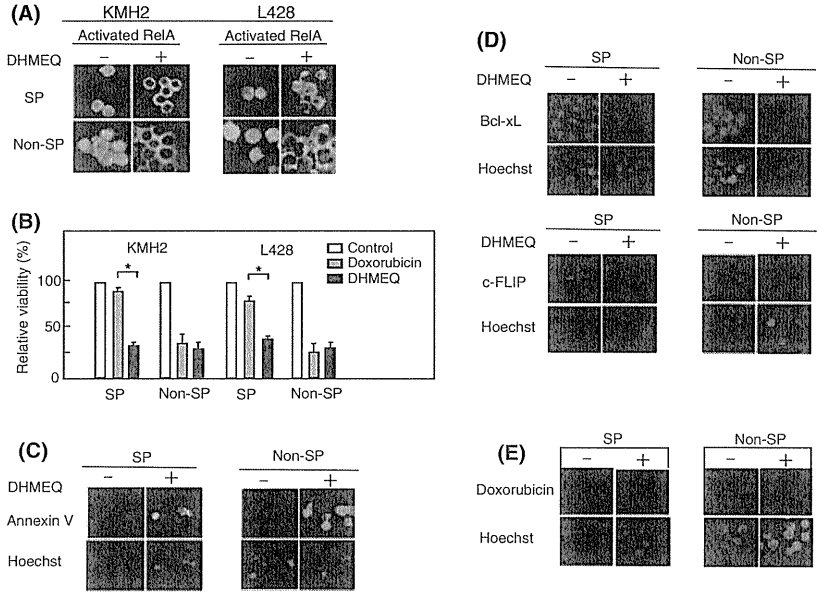

Fig. 5. Effect of dehydroxymethylepoxyquinomicin (DHMEQ) and doxorubicin on side population (SP) and non-SP cells. (A) DHMEQ inhibits constitutive nuclear factor-κB activity in both SP and non-SP cells. The SP and non-SP cells were treated with 20 μg/mL DHMEQ for 6 h. The treated cells were stained for activated nuclear factor-κB (RelA). (B) DHMEQ reduces the viability of SP cells resistant to doxorubicin. Two thousand of cells were treated with 20 μg/mL DHMEQ or 1 μg/mL doxorubicin for 24 h. Viable cells were measured using the Trypan blue exclusion test and expressed as a percentage relative to the DMSO-treated control, which assigned a value of 100%. Data are the means ± SD of three independent experiments. $*P < 0.05$. (C) The DHMEQ-mediated reduction in cell viability is accompanied by an increase in the number of annexin V-reactive cells. Cells were separated then treated with 20 μg/mL DHMEQ for 18 h, stained with annexin V, and observed. Detection of Hoechst varied between SP and non-SP cells, because of the very weak signal in the SP cells. (D) DHMEQ inhibits the expression of Bcl-xL and c-FLIP in both SP and non-SP cells. The SP and non-SP cells were treated with 20 μg/mL DHMEQ or DMSO alone for 7 h. The treated cells and their control were stained for Bcl-xL and c-FLIP. Isotype-matched control antibody showed negative staining (data not shown). Detection of Hoechst was varied. (E) Incorporation of doxorubicin into SP and non-SP cells. Cells were cultured for 1 h with 1 μg/mL doxorubicin under the same conditions as Figure (5B). The cells were observed using a fluorescence microscope with a WIG filter (Olympus) on an Olympus BX50F fluorescence microscope. Detection of Hoechst was varied.

from the $CD30^-$ fraction in KMH2 and L428 cell lines and the $CD30^+$ fraction is not yet analyzed. Our study indicates the presence of precursor cells within the $CD30^+$ fraction and emphasizes the requirement of further study of this fraction.

We have shown that CD30 is overexpressed in HL and that overexpressed CD30 induces ligand-independent signals.[6] These signals drive constitutive NF-κB activation that is critical for the survival of HL cells, and also induce the expression of JunB, which is responsible for positive regulation of CD30 overexpression through AP-1 activation.[6,7] Although chemotherapy and radiotherapy successfully contribute to a better prognosis of HL, problems of late side-effects and cases resistant to the treatment with poor prognosis, are also important issues that remain to be solved.[28] As SP cells, which share characteristics of CSCs, are considered to be associated with resistance to chemotherapy,[29] successful targeting of this fraction appears to be critical for eradication of HL cells. We showed that the SP cells are resistant to doxorubicin, a key conventional chemotherapeutic agent for HL, whereas the SP cells are sensitive to NF-κB inhibitor DHMEQ. We indicated that DHMEQ induced apoptosis in not only non-SP cells, but also in SP cells by downregulation of anti-apoptotic molecules, Bcl-xL and c-FLIP. Although the SP cells showed resistance for doxorubicin, doxorubicin was incorporated into their nucleus. The results indicated that the resistance of the SP to doxorubicin was not due to increased efflux by transporters. Taking into account the fact that the SP of KMH2 is actively replicating, the resistance to doxorubicin does not relate to the quiescent nature of cells, but might therefore be due to altered intracellular metabolism or signaling, which may be distinct compared to non-SP cells.[30,31] Taken collectively, these results underscore the significance of NF-κB inhibition to eradicate HL cells.

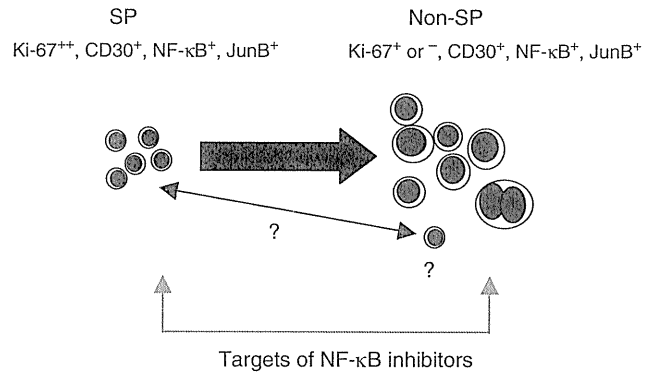

Fig. 6. Proposed model for the roles of the small mononuclear cells found in the side population (SP). The small mononuclear cells in the SP proliferate actively and generate the non-SP, consisting of larger cells with Hodgkin or Reed-Sternberg cell-like morphology. Part of the non-SP cells is not actively replicating. The SP may be linked with the non-SP by a very small fraction of cells that exist in the non-SP. The biological bases of Hodgkin's lymphoma previously reported appear to be conserved and nuclear factor (NF)-κB is a molecular target for both populations.

In conclusion, our results indicate that HL cell lines contain an SP and typical small mononuclear cells enriched in this SP appear to be a certain stage of precursor cells for H and RS cells. A population of non-SP cells, which link the non-SP and SP, may exist. The biological bases characteristic for HL appear to be shared between the SP and non-SP cells. The results also present an example of NF-κB as a key signaling pathway for the SP cells and stress the significance of NF-κB inhibition for

doi: 10.1111/j.1349-7006.2010.01693.x

eradication of HL cells. A schematic representation of the conclusion is presented as Figure 6.

Acknowledgments

This work was supported in part by Grants-in Aid from the Graduate School of Medical Sciences, Kitasato University (Sagamihara, Japan) and from the Ministry of Education, Science, and Culture of Japan to R.H., and Grants-in-Aid from the Ministry of Health, Labor, and Welfare of Japan for the Third-term Comprehensive 10-year Strategy for Cancer Control and for Cancer Research to TW.

References

1 Gruss HJ, Kadin ME. Pathophysiology of Hodgkin's disease: functional and molecular aspects. *Baillieres Clin Haematol* 1996; **9**: 417–46.
2 Kuppers R, Kanzler H, Hansmann ML, Rajewsky K. Single cell analysis of Hodgkin/Reed-Sternberg cells. *Ann Oncol* 1996; **7**(Suppl 4): 27–30.
3 Drexler HG, Gignac SM, Hoffbrand AV, Minowada J. Formation of multinucleated cells in a Hodgkin's-disease-derived cell line. *Int J Cancer* 1989; **43**: 1083–90.
4 Horie R, Watanabe T. CD30: expression and function in health and disease. *Semin Immunol* 1998; **10**: 457–70.
5 Horie R, Watanabe T. The biological basis of Hodgkin's lymphoma. *Drug News Perspect* 2003; **16**: 649–56.
6 Horie R, Watanabe T, Morishita Y *et al.* Ligand-independent signaling by overexpressed CD30 drives NF-kappaB activation in Hodgkin-Reed-Sternberg cells. *Oncogene* 2002; **21**: 2493–503.
7 Watanabe M, Sasaki M, Itoh K *et al.* JunB induced by constitutive CD30-extracellular signal-regulated kinase 1/2 mitogen-activated protein kinase signaling activates the CD30 promoter in anaplastic large cell lymphoma and reed-sternberg cells of Hodgkin lymphoma. *Cancer Res* 2005; **65**: 7628–34.
8 Reya T, Morrison SJ, Clarke MF, Weissman IL. Stem cells, cancer, and cancer stem cells. *Nature* 2001; **414**: 105–11.
9 Cho RW, Clarke MF. Recent advances in cancer stem cells. *Curr Opin Genet Dev* 2008; **18**: 48–53.
10 Hirschmann-Jax C, Foster AE, Wulf GG *et al.* A distinct ''side population'' of cells with high drug efflux capacity in human tumor cells. *Proc Natl Acad Sci U S A* 2004; **101**: 14228–33.
11 Zhou S, Schuetz JD, Bunting KD *et al.* The ABC transporter Bcrp1/ABCG2 is expressed in a wide variety of stem cells and is a molecular determinant of the side-population phenotype. *Nat Med* 2001; **7**: 1028–34.
12 Wu C, Alman BA. Side population cells in human cancers. *Cancer Lett* 2008; **268**: 1–9.
13 Newcom SR, Kadin ME, Phillips C. L-428 Reed-Sternberg cells and mononuclear Hodgkin's cells arise from a single cloned mononuclear cell. *Int J Cell Cloning* 1988; **6**: 417–31.
14 Watanabe M, Nakashima M, Togano T *et al.* Identification of the RelA domain responsible for action of a new NF-kappaB inhibitor DHMEQ. *Biochem Biophys Res Commun* 2008; **376**: 310–4.
15 Watanabe M, Dewan MZ, Taira M *et al.* IkappaBalpha independent induction of NF-kappaB and its inhibition by DHMEQ in Hodgkin/Reed-Sternberg cells. *Lab Invest* 2007; **87**: 372–82.
16 Jones KH, Senft JA. An improved method to determine cell viability by simultaneous staining with fluorescein diacetate-propidium iodide. *J Histochem Cytochem* 1985; **33**: 77–9.
17 Wan G, Zhou L, Xie M, Chen H, Tian J. Characterization of side population cells from laryngeal cancer cell lines. Head Neck 2010; doi:10.1002/hed.21325.
18 Mitsutake N, Iwao A, Nagai K *et al.* Characterization of side population in thyroid cancer cell lines: cancer stem-like cells are enriched partly but not exclusively. *Endocrinology* 2007; **148**: 1797–803.
19 Patrawala L, Calhoun T, Schneider-Broussard R, Zhou J, Claypool K, Tang DG. Side population is enriched in tumorigenic, stem-like cancer cells, whereas ABCG2 + and ABCG2- cancer cells are similarly tumorigenic. *Cancer Res* 2005; **65**: 6207–19.
20 Sales KM, Winslet MC, Seifalian AM. Stem cells and cancer: an overview. *Stem Cell Rev* 2007; **3**: 249–55.
21 Umezawa K. Inhibition of tumor growth by NF-kappaB inhibitors. *Cancer Sci* 2006; **97**: 990–5.
22 Kim LH, Nadarajah VS, Peh SC, Poppema S. Expression of Bcl-2 family members and presence of Epstein-Barr virus in the regulation of cell growth and death in classical Hodgkin's lymphoma. *Histopathology* 2004; **44**: 257–67.
23 Thomas RK, Kallenborn A, Wickenhauser C *et al.* Constitutive expression of c-FLIP in Hodgkin and Reed-Sternberg cells. *Am J Pathol* 2002; **160**: 1521–8.
24 Addla SK, Brown MD, Hart CA, Ramani VA, Clarke NW. Characterization of the Hoechst 33342 side population from normal and malignant human renal epithelial cells. *Am J Physiol Renal Physiol* 2008; **295**: F680–7.
25 Loebinger MR, Giangreco A, Groot KR *et al.* Squamous cell cancers contain a side population of stem-like cells that are made chemosensitive by ABC transporter blockade. *Br J Cancer* 2008; **98**: 380–7.
26 Jones RJ, Gocke CD, Kasamon YL *et al.* Circulating clonotypic B cells in classic Hodgkin lymphoma. *Blood* 2009; **113**: 5920–6.
27 Kuppers R. Clonotypic B cells in classic Hodgkin lymphoma. *Blood* 2009; **114**: 3970–1; author reply 1–2.
28 Diehl V. Chemotherapy or combined modality treatment: the optimal treatment for Hodgkin's disease. *J Clin Oncol* 2004; **22**: 15–8.
29 Dean M, Fojo T, Bates S. Tumour stem cells and drug resistance. *Nat Rev Cancer* 2005; **5**: 275–84.
30 Keenan J, Murphy L, Henry M, Meleady P, Clynes M. Proteomic analysis of multidrug-resistance mechanisms in adriamycin-resistant variants of DLKP, a squamous lung cancer cell line. *Proteomics* 2009; **9**: 1556–66.
31 Shim GS, Manandhar S, Shin DH, Kim TH, Kwak MK. Acquisition of doxorubicin resistance in ovarian carcinoma cells accompanies activation of the NRF2 pathway. *Free Radic Biol Med* 2009; **47**: 1619–31.

Supporting Information

Additional Supporting Information may be found in the online version of this article.

Fig. S1. Overlaid histograms of each marker. The expression was analyzed by FACSAria using each antibody (light blue, right peak of each plot) or a control antibody (light grey, left peak of each plot). The horizontal axis indicates fluorescence intensity, the vertical axis represents cell count (% of maximum).

Please note: Wiley-Blackwell are not responsible for the content or functionality of any supporting materials supplied by the authors. Any queries (other than missing material) should be directed to the corresponding author for the article.

Oncogene (2010) 29, 4157–4169

www.nature.com/onc

ORIGINAL ARTICLE

Downregulation of ZEB1 and overexpression of Smad7 contribute to resistance to TGF-β1-mediated growth suppression in adult T-cell leukemia/lymphoma

S Nakahata[1], S Yamazaki[2], H Nakauchi[2] and K Morishita[1]

[1]*Division of Tumor and Cellular Biochemistry, Department of Medical Sciences, Faculty of Medicine, University of Miyazaki, Miyazaki, Japan and* [2]*Laboratory of Stem Cell Therapy, Center for Experimental Medicine, The Institute of Medical Science, University of Tokyo, Tokyo, Japan*

Zinc-finger E-box binding homeobox 1 (*ZEB1*) is a candidate tumor-suppressor gene in adult T-cell leukemia/lymphoma (ATLL). *ZEB1* binds phosphorylated Smad2/3 to enhance transforming growth factor-β1 (TGF-β1) signaling. In addition to downregulation of *ZEB1* mRNA, we found overexpression of inhibitory Smad, Smad7, in resistance of ATLL cells to growth suppression by TGF-β1. A protein complex of Smad7 and histone deacetylase constantly bound to the promoter region of TGF-β1 responsive genes with the Smad-responsive element (SRE) to inhibit TGF-β1 signaling; however, ectopic expression of ZEB1 reactivated TGF-β1 signaling by binding to Smad7 and recruiting the Smad3/p300 histone acetyltransferase complex to the promoter after TGF-β1 stimulation in ATLL. Conversely, because *ZEB1* mRNA was detected in the late stages of T-cell development, we used CTLL2 cells with *ZEB1* expression, a murine peripheral T-cell lymphoma, and found that a complex of Smad3, Smad7 and ZEB1 was bound to the SRE of the *p21*^{CDKN1A} promoter after the induction of Smad7 by TGF-β1 treatment. Because the duration of TGF-β1-induced transcriptional activation of *PAI-1* and *p21* was shortened in shZEB1-expressing CTLL2 cells, ZEB1 may have a role in enhancing TGF-β1 signaling by binding not only to Smad3 but also to Smad7 in the nucleus. Altogether, these results suggest that both ZEB1 downregulation and Smad7 overexpression contribute to resistance to TGF-β1-mediated growth suppression in ATLL.
Oncogene (2010) **29,** 4157–4169; doi:10.1038/onc.2010.172; published online 31 May 2010

Keywords: ZEB1; Smad7; ATLL

Introduction

Adult T-cell leukemia/lymphoma (ATLL) is a malignant and fatal disorder of CD4$^+$ T cells that is caused by infection of these cells with human T-cell leukemia virus type I (HTLV-1). ATLL occurs in 3–5% of HTLV-1 carriers following a long latency period, which can range from 40 to 60 years (Yasunaga and Matsuoka, 2003). ATLL cells are derived from the malignant clonal expansion of an HTLV-1-infected CD4$^+$ T lymphocyte that has accumulated genetic lesions, including the activation of oncogenes or inactivation of tumor-suppressor genes (Tsukasaki *et al.*, 2001). A previous study from our laboratory discovered these genetic lesions by spectral karyotyping with a high-density single-nucleotide polymorphism array and comparative genomic hybridization in ATLL; we found that the T-cell transcription factor (TCF8)/zinc-finger E-box binding homeobox 1 (ZEB1) was a candidate tumor suppressor in ATLL (Hidaka *et al.*, 2008).

Transcription factors from the ZEB family have been characterized as downstream effectors of the transforming growth factor-β (TGF-β) signaling pathway. ZEB1 binds to receptor-regulated Smad2/3 and synergizes with Smad-mediated transcriptional activation (van Grunsven *et al.*, 2001; Postigo, 2003). TGF-β1 belongs to a superfamily of cytokines that regulates a broad range of cellular responses, including cell proliferation, differentiation, adhesion, migration and apoptosis (Kingsley, 1994). Deregulated TGF-β1 signaling has been implicated in various human diseases, including autoimmune diseases, vascular disorders and cancer (Blobe *et al.*, 2000). TGF-β1 has antiproliferative effects in a variety of cell types, and this negative regulation of cellular proliferation by TGF-β1 functions to suppress the growth of tumor cells (Derynck *et al.*, 2001). However, HTLV-1-infected T cells and ATLL cells are resistant to the growth inhibitory action of TGF-β1, even though these cells express high levels of TGF-β1 (Kim *et al.*, 1990). Although Tax, a viral protein, has been reported to render cells resistant to TGF-β1-mediated growth suppression (Mori *et al.*, 2001; Arnulf *et al.*, 2002), Tax expression is not detectable in most ATLL cells. Therefore, it has been suggested that ATLL cells develop different mechanisms of resistance to escape the antiproliferative signal that is mediated by TGF-β1. One such mechanism might be associated with aberrant expression of MEL1S (Yoshida *et al.*, 2004), which was originally isolated as the gene that was transcriptionally activated by t(1;3)(p36;q21) in acute myeloid leukemia

Correspondence: Dr K Morishita, Division of Tumor and Cellular Biochemistry, Department of Medical Sciences, Faculty of Medicine, University of Miyazaki, 5200 Kihara, Kiyotake, Miyazaki 889-1692, Japan.
E-mail: kmorishi@med.miyazaki-u.ac.jp
Received 19 October 2009; revised 3 March 2010; accepted 19 April 2010; published online 31 May 2010

(Mochizuki *et al.*, 2000). We previously reported that *ZEB1* expression was downregulated in a majority of ATLL cells (Hidaka *et al.*, 2008). Furthermore, *ZEB1*-mutant mice frequently developed $CD4^+$ T-cell lymphomas and/or leukemias, suggesting that *ZEB1* may have a tumor suppressive role in ATLL. In addition, the enforced expression of ZEB1 partially restored the responsiveness of ATLL cells to TGF-β1. Therefore, the downregulation of *ZEB1* expression may be associated with resistance to the growth inhibitory activity of TGF-β1.

In this paper, we report that Smad7, an inhibitory Smad (I-Smad), is overexpressed in HTLV-1-infected T-cell lines and primary leukemia cells from acute-type ATLL patients. Smad7 is immediately induced after TGF-β stimulation and acts as an antagonist of TGF-β signaling, which may regulate the intensity or duration of its signaling cascade (Shi and Massagué, 2003). Although constitutive expression of Smad7 inhibited TGF-β1 growth suppression in ATLL cells, we found that ectopically expressed ZEB1 overcame the Smad7-mediated inhibition of TGF-β1 signaling. Smad7 constitutively bound to the promoter of the TGF-β1 responsive genes with the Smad-responsive element (SRE) to inhibit TGF-β1 signaling. TGF-β1 stimulation, in the presence of ZEB1 overexpression, led to ZEB1 recruitment of the Smad3 complex to the promoter region with Smad7 to reactivate TGF-β1 signaling. Conversely, *ZEB1* mRNA was expressed in $CD4^+CD8^+$, $CD4^+CD8^-$ and $CD4^-CD8^+$ T cells in the late stages of T-cell development, and using CTLL2, a murine T-lymphoma cell line with *ZEB1* expression, we examined the protein complexes associated with the promoter region of the TGF-β1 responsive genes with SRE and time course for gene expression of the TGF-β1 activating genes *Smad6*, *Smad7*, plasminogen activator inhibitor 1 (*PAI-1*) and cyclin-dependent kinase inhibitor 1A (*p21*). We found that a ternary complex of Smad3, Smad7 and ZEB1 on the *p21* promoter with the SRE kept activating *p21* transcription after the induction of Smad7 by TGF-β1. TGF-β1 stimulation of CTLL2 cells expressing a short hairpin to ZEB1 led to a shorter expression time interval of *PAI-1* and *p21* whereas the expression of *Smad6* and *Smad7* remained unchanged. The results suggest that ZEB1 enhances TGF-β1 signaling by binding not only to the Smad3 complex and but also to Smad7 in the nucleus. Thus, ZEB1 may have important roles in the regulation of TGF-β1 signaling, and both ZEB1 downregulation and Smad7 overexpression may be important molecular events that contribute to resistance to TGF-β1 signaling in ATLL.

Results

Upregulated expression of I-Smad7 in ATLL cells

We previously reported that *ZEB1* expression was downregulated and functioned as a possible tumor suppressor in a majority of ATLL cells (Hidaka *et al.*, 2008). ZEB1 has been reported to bind Smad3 and enhance TGF-β1 signaling, and the resistance of HTLV-1-infected T cells and ATLL cells to TGF-β1-mediated growth inhibition is one of the most prominent characteristics of ATLL. Because ectopic expression of ZEB1 in ATLL cells partially restored sensitivity to TGF-β1, the mRNA expression of four Smad family members (Smad2, 3, 6 and 7) that function as modulators of TGF-β1 signaling were analyzed using semiquantitative RT–PCR in four HTLV-1-negative T-acute lymphoblastic leukemia (T-ALL) cell lines (MOLT4, MKB1, KAWAI and Jurkat) (referred as HTLV-1 (−)) and seven HTLV-1-positive cell lines (HTLV-1 (+)). These HTLV-1 (+) cell lines included two HTLV-1-infected cell lines (MT2 and Hut102) and five ATLL-derived cell lines (ED, KOB, SO4, KK1 and S1T) (Figure 1a). The MOLT4 cells and all seven HTLV-1 (+) cell lines had high expression of inhibitory *Smad7*, but not of *Smad6* mRNA, whereas the other three HTLV-1 (−) cell lines (MKB-1, KAWAI and Jurkat) did not express *Smad7* but expressed *Smad6*. In addition, there were no significant differences in the pattern of *Smad2* and *Smad3* expression between the HTLV-1 (−) and HTLV-1 (+) cell lines. Because *HTLV-1 tax/rex* mRNA was expressed in two HTLV-1-infected cell lines (MT2 and Hut102) and two ATLL-derived cell lines (KOB and SO4), the expression patterns of *HTLV-1 tax/rex* did not appear to correlate with the expression of the four members of the Smad family. To confirm that protein levels of ZEB1, Smad3 and Smad7 correlate with the mRNA level in the leukemia cell lines, we analyzed protein expression by western blot (Supplementary Figure 1). In HTLV-1 (+) cells, we detected a significantly higher and lower expression level of Smad7 and ZEB1 mRNA and protein, respectively, compared to HTLV-1 (−) cells.

Next, we used real-time RT–PCR analysis to determine the quantitative expression levels of *Smad7* and *ZEB1* in the same 11 cell lines. The expression of *Smad7* mRNA in the HTLV-1 (+) cell lines and the MOLT4 cell line was significantly higher ($P<0.05$) than in the HTLV-1 (−) cell lines. However, the expression of *ZEB1* mRNA was significantly reduced in the HTLV-1 (+) cell lines (Figure 1b). The *Smad7*/*ZEB1* expression ratio was 10-fold greater in the HTLV-1 (+) cell lines and the MOLT4 cell line compared to the $CD4^+$ T lymphocytes from normal volunteers. To confirm the expression pattern of high Smad7 with low ZEB1 in ATLL cells from patient samples, we used real-time RT–PCR using RNA isolated from ATLL cells derived from eight acute-type ATLL patients and normal $CD4^+$ T lymphocytes. As observed with the cell lines, all ATLL cells from patients with acute-type ATLL had higher Smad7/ZEB1 ratios than the $CD4^+$ T lymphocytes from normal volunteers ($P<0.05$) (Figure 1c). In two patients (no. 4 and 7), the expression of Smad7 was almost equal to the level in normal $CD4^+$ T cells; however, the expression of ZEB1 was clearly decreased, suggesting that the reduction of ZEB1 may contribute to a part of the resistance to TGF-β1 signaling. Alternatively, *Smad6* was weakly expressed in one out of eight ATLL cells and was not expressed in the $CD4^+$ T lymphocytes from normal volunteers (Supplementary Figure 2). Therefore, these data suggest that the higher expression

of I-Smad7 and downregulation of ZEB1 in ATLL cells could potentially modulate the responsiveness to TGF-β1-mediated growth suppression in ATLL cells.

Constitutive expression of Smad7 in ATLL cells renders cells resistant to TGF-β1-mediated growth inhibition

To assess whether the expression levels of ZEB1 and Smad7 could modulate TGF-β1 growth suppression in T-lymphoid cell lines, we downregulated endogenous *Smad7* and *ZEB1* expression in the MOLT4 cell line by transfecting an shRNA expression vector pSIREN-RetroQ-ZsGreen (Clontech, Mountain View, CA, USA) for Smad7 (shSmad7) and/or ZEB1 (shZEB1), as well as one for firefly luciferase, which served as a control (shLuc). Downregulation of *Smad7* and/or *ZEB1* expression was confirmed by semiquantitative (left, Figure 2a) and quantitative RT–PCR (Figure 2b). Approximately 70% of the parental and MOLT4-shLuc cells survived treatment with 10 ng/ml TGF-β1 for 48 h, the maximal inhibitory concentration (right, Figure 2a). In response to treatment with 10 ng/ml TGF-β1, 37% of the MOLT4-shSmad7 and 87% of the MOLT4-shZEB1 cells survived. Approximately 52% of shSmad7/shZEB1-transfected MOLT4 (MOLT4-shZEB1 + shSmad7) survived the TGF-β1 treatment, placing the survival rate of this cell line between the parental-MOLT4-shLuc and MOLT4-shSmad7 cells. We plotted the expression ratio of Smad7 and ZEB1 against the percentages of cell survival after the TGF-β1 treatment in the context of the various transfection conditions for the MOLT4 cell lines. As shown in Figure 2b, the survival rates of TGF-β1 treated MOLT4 cells, with the exception of MOLT4-shZEB1, correlated significantly with the expression ratios of Smad7 and ZEB1 ($R^2 = 0.9682$). Almost all of the HTLV-1 (+) cell lines with significantly high-expression ratios had a similar survival rate of nearly 100% ($R^2 = 0.7333$), suggesting that cell lines with an expression ratio of Smad7/ZEB1 of more than 20-fold have a nearly 100% survival rate after TGF-β1 treatment.

To confirm whether the elevated Smad7 expression had a role in the resistance to TGF-β1 growth inhibition of HTLV-1 (+) cell lines irrespective of Tax expression, we downregulated endogenous Smad7 in Tax-positive MT2 and Tax-negative KK1 cell lines by transfection of a vector expressing shSmad7. The growth of the shSmad7-transfected MT2 and KK1 cells was inhibited by TGF-β1 treatment for 48 h in a dose-dependent manner, whereas both of the parental cells and the control shLuc-transfected cells were completely resistant to the growth inhibitory action of TGF-β1 (Figures 2c and d). In both the Tax-positive cell lines (MT2 and Hut102; Supplementary Figure 3) and the Tax-negative cell lines (MOLT4 and KK1), shSmad7 transfection

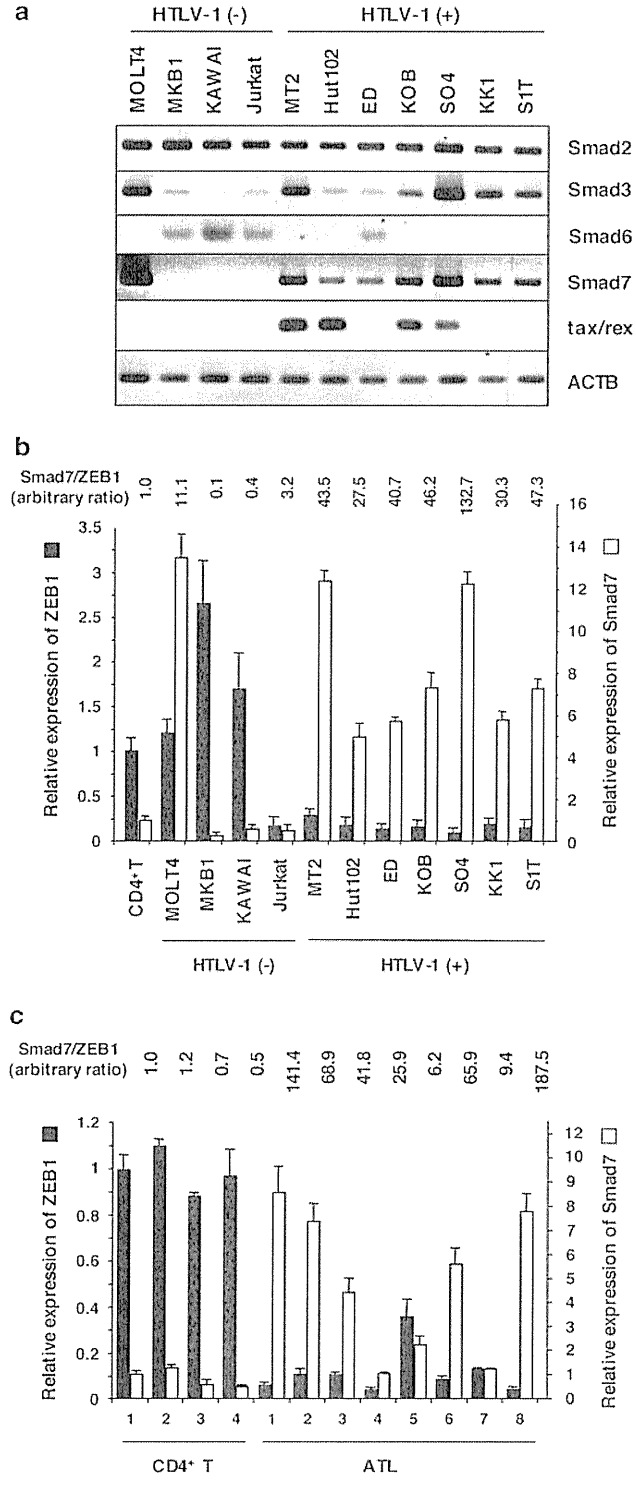

Figure 1 The mRNA expression profile of the Smad family. (**a**) Semiquantitative RT–PCR analysis for *Smad2*, *Smad3*, *Smad6*, *Smad7* and *HTLV-1 tax/rex* is shown in four HTLV-1-negative (MOLT4, MKB1, KAWAI and Jurkat) and seven HTLV-1-positive (MT2, Hut102, ED, KOB, SO4, KK1 and S1T) cell lines. The expression of β-actin (*ACTB*) is shown at the bottom as a control. (**b**) Quantitative RT–PCR analysis for *Smad7* and *ZEB1* is shown in the four HTLV-1-negative and seven HTLV-1-positive cell lines. *Smad7* and *ZEB1* mRNA expression levels were normalized to β-actin mRNA expression and expressed relative to the mRNA level in a healthy control (CD4 + T). The relative levels of *Smad7* and *ZEB1* expression are presented as a ratio of *Smad7*/*ZEB1* mRNA. Student's *t*-test was used for the statistical analysis. (**c**) Quantitative RT–PCR analysis for *Smad7* and *ZEB1* is shown in eight patients with acute-type ATLL (ATL) and in four healthy controls (CD4 + T). *Smad7* and *ZEB1* mRNA expression levels were expressed relative to the mRNA level in a healthy control. The data are presented as in Figure 1b.

enhanced the growth-suppression effect of TGF-β1. In addition, enforced expression of ZEB1 in many HTLV-1 (+) cell lines enhanced TGF-β1 growth suppression, suggesting that Tax expression was independent of the modulation of TGF-β1 responsiveness by *Smad7* and *ZEB1* expression.

ZEB1 counteracts Smad7 repression of TGF-β1 signal transduction

To determine how the expression of Smad6, Smad7 and/or ZEB1 is involved in TGF-β1 signaling, we assayed the activity of the promoter in HepG2 hepatocellular carcinoma cells using a luciferase reporter plasmid with the TGF-β1-responsive elements from the *PAI-1* promoter (p3TP-Lux). Co-transfection of Smad6 with the 3TP-Lux promoter vector weakly inhibited the TGF-β1-induced transcriptional activity, and co-transfection of Smad7 significantly inhibited TGF-β1-induced transcription (Figure 3a). Co-transfection of ZEB1 alone enhanced the TGF-β1-induced 3TP-Lux promoter activity (Figure 3b), probably through a direct interaction with Smad3 (Postigo, 2003). Importantly, co-transfection of ZEB1 with Smad6 or Smad7 overcame the inhibition of TGF-β1 signaling in a dose-dependent manner (Figure 3b). These results suggest that ZEB1 might counteract the Smad6- and Smad7-mediated inhibition of TGF-β1 growth suppression.

To determine the physical interaction between ZEB1 and I-Smad proteins, we performed co-immunoprecipitation experiments using 293T cells that were transiently transfected with ZEB1 and FLAG-tagged Smad6 or Smad7 expression plasmids. As shown in Figure 3c, ZEB1 coprecipitated with Smad6 or Smad7, indicating that ZEB1 could interact with both of the I-Smad proteins. To assess whether ZEB1 could directly modulate the Smad7-mediated inhibition of TGF-β1 signaling in ATLL cells, we evaluated the protein interaction and subcellular localization of endogenous ZEB1 and Smad7 proteins. To detect the physical interaction of endogenous ZEB1 with Smad7 or Smad3, we immunoprecipitated whole-cell lysates from MOLT4 cells treated with or without TGF-β1 for 24 h with an anti-ZEB1 antibody, and the immune complexes were

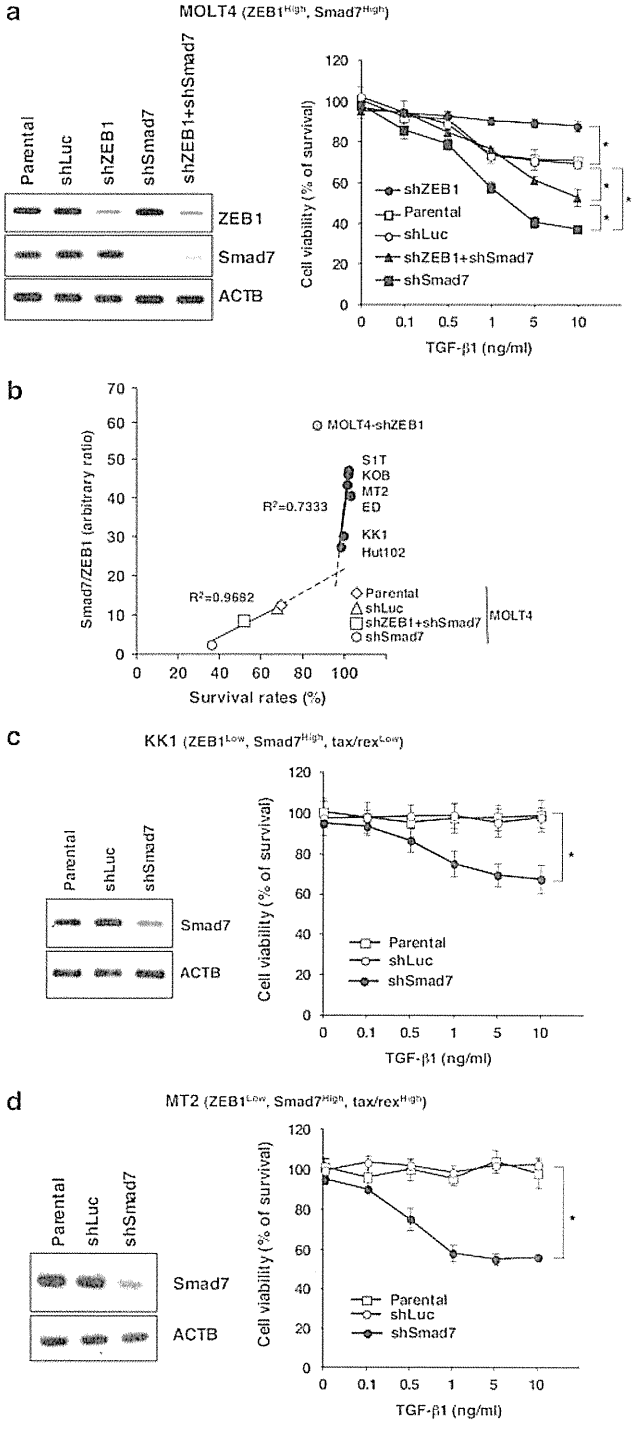

Figure 2 Correlation between expression levels of Smad7 and ZEB1 and responsiveness to TGF-β1. (**a**) Effect of downregulation of endogenous Smad7 and ZEB1 on TGF-β1-induced growth inhibition in MOLT4 cells. (Left) Semiquantitative RT–PCR analysis was performed with mRNA isolated from MOLT4 cells that were either untransfected (Parental) or transfected with the control luciferase-specific shRNA (shLuc), the Smad7-specific shRNA (shSmad7), the ZEB1-specific shRNA (shZEB1) or both the ZEB1- and Smad7-specific shRNA vectors (shZEB1 + shSmad7). PCR for *Smad7*, *ZEB1* and β-actin are shown. (Right) Viable cells after treatment with the indicated concentration of TGF-β1 for 48 h were examined using the MTT assay and are shown as the percentages of the values obtained from the unstimulated parental cells. The cell number per ml at time zero was 4×10^4. Student's *t*-test was used for the statistical analysis, and $P < 0.05$ (asterisk) was considered significant. (**b**) Correlation between the expression ratios of *Smad7* and *ZEB1* and cell survival rates after TGF-β1 treatment in various transfected MOLT4 cells versus various HTLV-1 (+) cell lines. Scatter plots with a smooth trend line are shown. The coefficient of correlation (R^2) is indicated for each trend line. (**c**, **d**) The effect of downregulation of endogenous Smad7 in TGF-β1-induced growth inhibition in Tax-non-expressing (**c**) and Tax-expressing (**d**) HTLV-1-positive cell lines. Semiquantitative RT–PCR analysis and viable cell counts were performed with KK1 and MT2 cells that were untransfected (Parental) or transfected with either the control luciferase-specific shRNA vector (shLuc) or the Smad7-specific shRNA vector (shSmad7). (Left) Semiquantitative RT–PCR for *Smad7* and β-actin mRNA are shown in each cell line. (Right) After transfection with the shRNA vectors, the cells were treated with the indicated concentration of TGF-β1 for 48 h. The degree of proliferation of each cell line was examined by MTT assay. The data are presented as in Figure 2a.

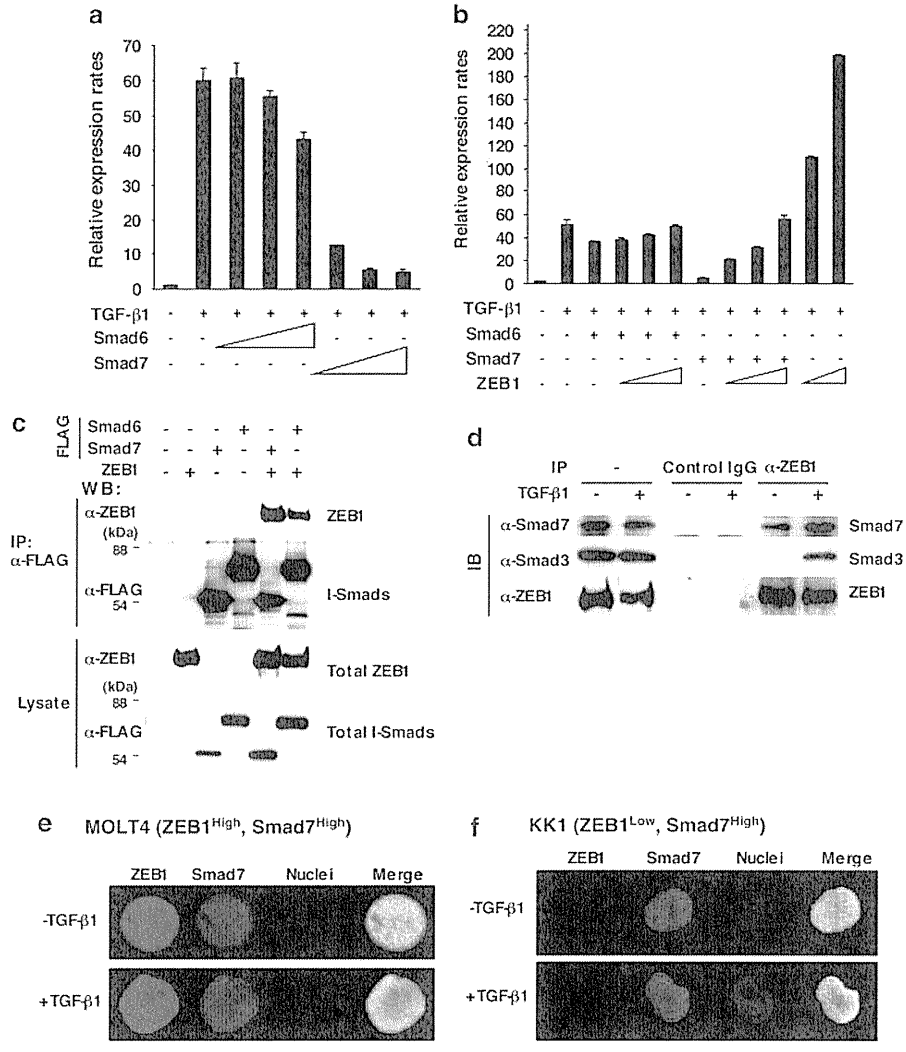

Figure 3 Counteraction of TGF-β1 signal transduction by ZEB1 and Smad7. (**a**) Smad7 expression significantly decreases the TGF-β1 responsiveness of a Smad-dependent gene promoter. 3TP-Lux reporter assays were performed in HepG2 cells with co-transfection of either control pcDNA3 (−), increasing amounts of FLAG-Smad7/pcDNA3 or FLAG-Smad6/pcDNA3, and 3TP-Lux reporter plasmid plus stimulation by 5 ng/ml of TGF-β1 (+) or phosphate-buffered saline (PBS) (−) for 24 h. The results are shown as the means and s.d. of triplicate transfections. The activity obtained in the absence of TGF-β1 was set at 1. (**b**) ZEB1 counteracts the inhibitory effects of Smad6 or Smad7. 3TP-Lux reporter assays were performed in HepG2 cells transiently transfected with pcDNA3 (−), FLAG-Smad6/pcDNA3 or FLAG-Smad7/pcDNA3, and/or increasing amounts of the ZEB1/pcDNA and 3TP-Lux reporter plasmids. Cells were stimulated with 5 ng/ml of TGF-β1 (+) or PBS (−) for 24 h. (**c**) ZEB1 interacts with Smad6 or Smad7. 293T cells were transiently transfected with ZEB1, FLAG-Smad7 and/or FLAG-Smad6 expression plasmids, and the whole-cell lysates were immunoprecipitated with an anti-FLAG antibody. The immunoprecipitates were detected by anti-ZEB1 or anti-FLAG antibody. (**d**) Endogenous ZEB1 interacts with endogenous Smad7 or Smad3 in MOLT4 cells. After treatment with 10 ng/ml of TGF-β1 or PBS as control for 24 h, whole-cell lysates from MOLT4 cells were immunoprecipitated with an anti-ZEB1 antibody. The immunoprecipitates were immunoblotted using anti-Smad7 or anti-Smad3 antibody. (**e**, **f**) Subcellular localization of ZEB1 and Smad7 in the absence or presence of TGF-β1 stimulation. After MOLT4 (**e**) and KK1 (**f**) cells were treated with 10 ng/ml of TGF-β1 (+TGF-β1) or PBS (−TGF-β1) for 24 h, localization of endogenous ZEB1 and Smad7 was detected by indirect immunofluorescence using anti-ZEB1 and anti-Smad7 antibodies. The proteins were visualized using an Alexa Fluor 488-conjugated anti-goat secondary antibody (green, for ZEB1) and the Alexa Fluor 555-conjugated anti-rabbit secondary antibody (red, for Smad7). The cells were analyzed using confocal microscopy, and the DAPI (4,6-diamidino-2-phenylindole) stain was used to visualize the nuclei.

subjected to immunoblot analysis using an anti-Smad3 or anti-Smad7 antibody (Figure 3d). The binding of ZEB1 to Smad3 was only detected in the presence of TGF-β1; however, Smad7 consistently co-precipitated with ZEB1 in both the absence and presence of TGF-β1.

Next, to confirm the interaction and subcellular localization of endogenous ZEB1 and Smad7 proteins, both proteins in MOLT4-TALL and KK1-HTLV1 (+) cell lines were immunostained with different fluorescent dyes with either anti-ZEB1 or anti-Smad7 antibody, and the labeled proteins were examined using a confocal microscope. The specificity of the antibody against Smad7 was evaluated by shRNA knockdown experiments. Smad7 was significantly reduced in the shSmad7-

treated cells but not in the shLuc-transfected cells by immunoblots and immunofluorescent staining (Supplementary Figure 4). In MOLT4 cells, ZEB1 and Smad7 were mainly colocalized in the nucleus (Figure 3e), confirming the protein interaction between endogenous ZEB1 and Smad7 (Figure 3d). Nuclear localization of Smad7 was also observed in the KK1-HTLV1 (+) cell line (Figure 3f). Therefore, ZEB1 may directly modulate the inhibitory function of Smad7 in the nucleus.

Association of ZEB1 with Smad7 or Smad3

To investigate the function of ZEB1 in the TGF-β1 signaling pathway, we initially examined the physical interactions between ZEB1, Smad3 and Smad7 with or without TGF-β1 treatment in HepG2 cells using immunoprecipitation and western blot. This was done because both the exogenously expressed ZEB1 and Smad7 were located in the nucleus regardless of TGF-β1 treatment (Supplementary Figure 5). In the absence of TGF-β1 treatment, neither the Smad3–ZEB1 nor Smad3–Smad7 interaction was observed by the coprecipitation assay using the corresponding specific antibody. After TGF-β1 treatment, Smad3 could be precipitated with ZEB1, but not with Smad7 (Supplementary Figure 6a). By contrast, Smad7 was constitutively associated with ZEB1 in HepG2 cells irrespective of TGF-β1 treatment (Supplementary Figure 6b). To identify the binding domain in Smad7 that was responsible for the interaction with ZEB1, we generated two Flag-tagged deletion mutants of Smad7: Smad7-N, which encoded the first half of Smad7 (amino acids 1–259), and Smad7-MH2, which encoded the second half of Smad7 containing the Mad-homology 2 (MH2) domain (amino acids 260–420) (Figure 4a). As shown in Figure 4b, ZEB1 did not coprecipitate with Smad7-N; however, ZEB1 did coprecipitate with Smad7-MH2. This suggests that ZEB1 interacts with the MH2 domain of Smad7. The Smad-interacting domain (SID) of ZEB1 has been reported to interact with Smad1, Smad2 or Smad3 in the nucleus after treatment with TGF-β1 (Postigo, 2003). Therefore, to determine which region of ZEB1 was necessary for binding to Smad7, three deletion mutant plasmids and a full-length *ZEB1* expression plasmid were generated (Figure 4a): a full-length ZEB1–GFP fusion construct (GFP-ZEB1), GFP fused to the N-terminal domain (amino acids 1–377; ZEB1-N), GFP fused to the SID (amino acids 378–457; ZEB1-SID) and GFP fused to the C-terminal domain (amino acids 458–1125; ZEB1-C). As shown in Figure 4c, only ZEB1-SID precipitated with Smad7 protein, suggesting that Smad7 interacts with the SID domain of ZEB1.

Because the SID region of ZEB1 interacts with both Smad3 and Smad7, it is possible that these two proteins compete for ZEB1 in the nucleus after TGF-β1 stimulation. To test this possibility, we transfected HepG2 cells with expression plasmids encoding three genes (*HA-Smad3*, *GFP-Smad7* and *FLAG-ZEB1*) in various combinations and treated with TGF-β1. As shown in Figure 4d, the ZEB1/Smad3, ZEB1/Smad7 and ZEB1/Smad3/Smad7 complexes could all be detected. The same interaction experiment was repeated with the difference being that the full-length *ZEB1* expression plasmid was replaced with a plasmid expressing solely the SID region of ZEB1 (GFP-ZEB1-SID). As shown in Supplementary Figure 7, the ZEB1-SID coprecipitated with Smad3, Smad7 and a complex of Smad3 and Smad7. Because Smad3 and Smad7 have not been shown to interact with each other, these data suggest that the SID region of ZEB1 may simultaneously interact with both Smad3 and Smad7. To assess this possibility, we immunoprecipitated lysates from cells transfected with HA-Smad3, FLAG-Smad7 and ZEB1 in the presence of TGF-β1 with either anti-HA or anti-FLAG antibody and coprecipitation of these three proteins was examined. As shown in Figure 4e, the ZEB1/Smad3/Smad7 complexes were identified in both anti-HA (Smad3) and anti-FLAG (Smad7) immunoprecipitates. We also performed a competitive binding experiment using cells that were co-transfected with a fixed amount of ZEB1-SID and Smad3 expression plasmids and increasing amounts of Smad7 expression plasmid (Figure 4f). After immunoprecipitation of GFP-ZEB1-SID, the ZEB1/SID/Smad3 complex could be detected regardless of the amount of Smad7 expression plasmid that was transfected into the cell. In the converse experiment, ZEB1/SID/Smad7 complex could be detected regardless of the amount of Smad3 expression plasmid that was transfected into the cells (Supplementary Figure 8). Therefore, regulatory Smad3 (R-Smad3) and I-Smad7 were able to bind to the ZEB1-SID region without competition.

Binding of the 3TP promoter region by a transcription factor complex of Smad3, Smad7 and ZEB1 after TGF-β1 stimulation

To investigate the transcriptional regulation by ZEB1 and the Smad proteins, we performed chromatin immunoprecipitation (ChIP) in HepG2 cells co-transfected with the p3TP-Lux and expression plasmids encoding HA-Smad3, FLAG-Smad7 and/or ZEB1. Formaldehyde crosslinked DNA isolated from transfected HepG2 cells was immunoprecipitated using the indicated antibody and subjected to semiquantitative PCR with primers specific for the 3TP promoter. After the transfection of HepG2 cells with the HA-Smad3 expression plasmid, we treated the cells with TGF-β1, and precipitated DNA fragments that bound to the protein complex with either an anti-HA (Smad3), anti-p300 or anti-HDAC1 antibody. Treatment with TGF-β1 induced a dramatic increase in the binding of the 3TP promoter region by both Smad3 and p300 (Figure 5a). Upon transfection of FLAG-Smad7 in either the absence or presence of TGF-β1, the Smad7 and HDAC1 complex was constantly bound to the 3TP promoter (Figure 5b). In addition, when HA-Smad3 and FLAG-Smad7 were co-transfected in the presence of TGF-β1 (Figure 5c), the Smad7/HDAC1 complex was found bound to the 3TP promoter; however, binding of the Smad3 and p300 complex to the promoter was

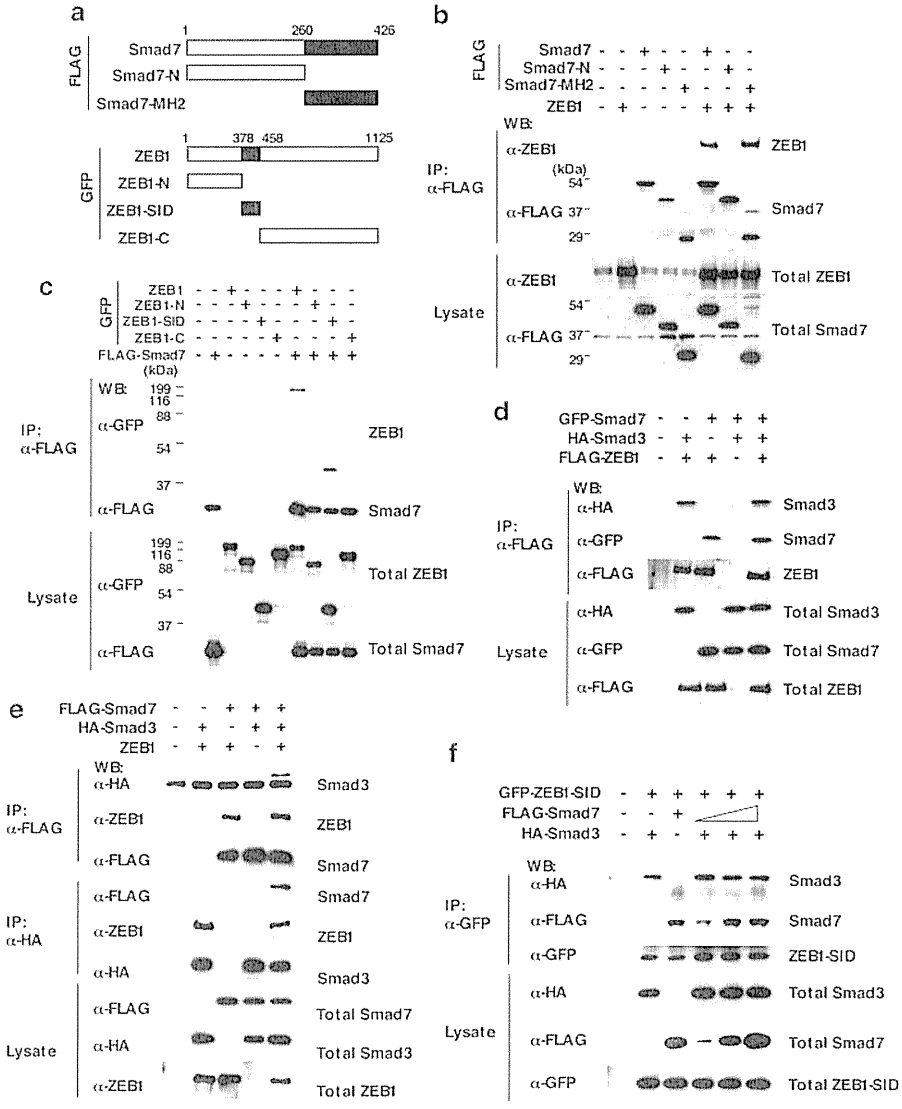

Figure 4 Mapping of the binding site involved in ZEB1/Smad complex formation. (**a**) Schematic representation of Smad7 and ZEB1. White bar indicates the C-terminal deletion mutant lacking the MH2 (Mad-homology 2) domain in Smad7 (Smad7-N). Black bar indicates the N-terminal deletion mutant of Smad7 (SMad7-MH2). The ZEB1-N mutant has 1–377 amino-acid residues before the Smad-interacting domain (SID), ZEB1-SID has the SID (378–457 aa), and the ZEB1-C mutant has the C-terminal region from SID (458–1125 aa). The numbers indicate the amino-acid residue. (**b**) The MH2 domain in Smad7 interacts with ZEB1. After transfection with expression vectors encoding FLAG-Smad7, FLAG-Smad7-N, FLAG-Smad7-MH2 and/or ZEB1 into 293T cells, cell lysates were immunoprecipitated with anti-FLAG antibody. The precipitates were immunoblotted with anti-ZEB1 or anti-FLAG antibody. (**c**) The SID domain in ZEB1 interacts with Smad7. After transfection with an expression vector encoding FLAG-Smad7 and/or various GFP-tagged ZEB1 constructs (Figure 4a) in 293T cells, the cell lysates were immunoprecipitated with anti-FLAG antibody. (**d**) ZEB1 interacts with Smad3 and Smad7. After transfection with FLAG-ZEB1, GFP-Smad7 and HA-Smad3 into HepG2 cells, the cells were treated with 5 ng/ml of TGF-β1 for 24 h. Cell lysates were precipitated by anti-FLAG antibody. The precipitates were immunoblotted by an anti-HA, anti-GFP or anti-FLAG antibody. (**e**) ZEB1 simultaneously interacts with both Smad3 and Smad7. After transfection with ZEB1, FLAG-Smad7, and HA-Smad3 into HepG2 cells, the cells were treated with 5 ng/ml of TGF-β1 for 24 h. Cell lysates were precipitated by either anti-FLAG or anti-HA antibody. The precipitates were immunoblotted by an anti-HA, anti-FLAG or anti-ZEB1 antibody. (**f**) Smad3 and Smad7 interact with ZEB1 in a noncompetitive manner. After transfection with GFP-ZEB1-SID, FLAG-Smad3 and/or increasing amounts of FLAG-Smad7 into HepG2 cells, the cells were treated with 5 ng/ml of TGF-β1 for 24 h and the cell lysates were immunoprecipitated with an anti-GFP antibody.

decreased. When cells were co-transfected with ZEB1, Smad3 and Smad7 in the presence of TGF-β1 (Figure 5d), the binding of Smad3 and p300 was clearly increased to similar levels as that seen with Smad3 transfection alone, while the occupancy of HDAC1 was decreased. The recruitment of ZEB1 to the 3TP promoter region is mediated by its interaction with Smad3 or Smad7, because no signal was detected when the cells were transfected with ZEB1 alone (Supplementary Figure 9). To examine whether *ZEB1* expression in HTLV-1 (+) cell lines results in the binding of the Smad7/ZEB1/Smad3/p300 complex to the 3TP promoter region following TGF-β1 stimulation, we performed ChIP in MT2 cells that were co-transfected with the

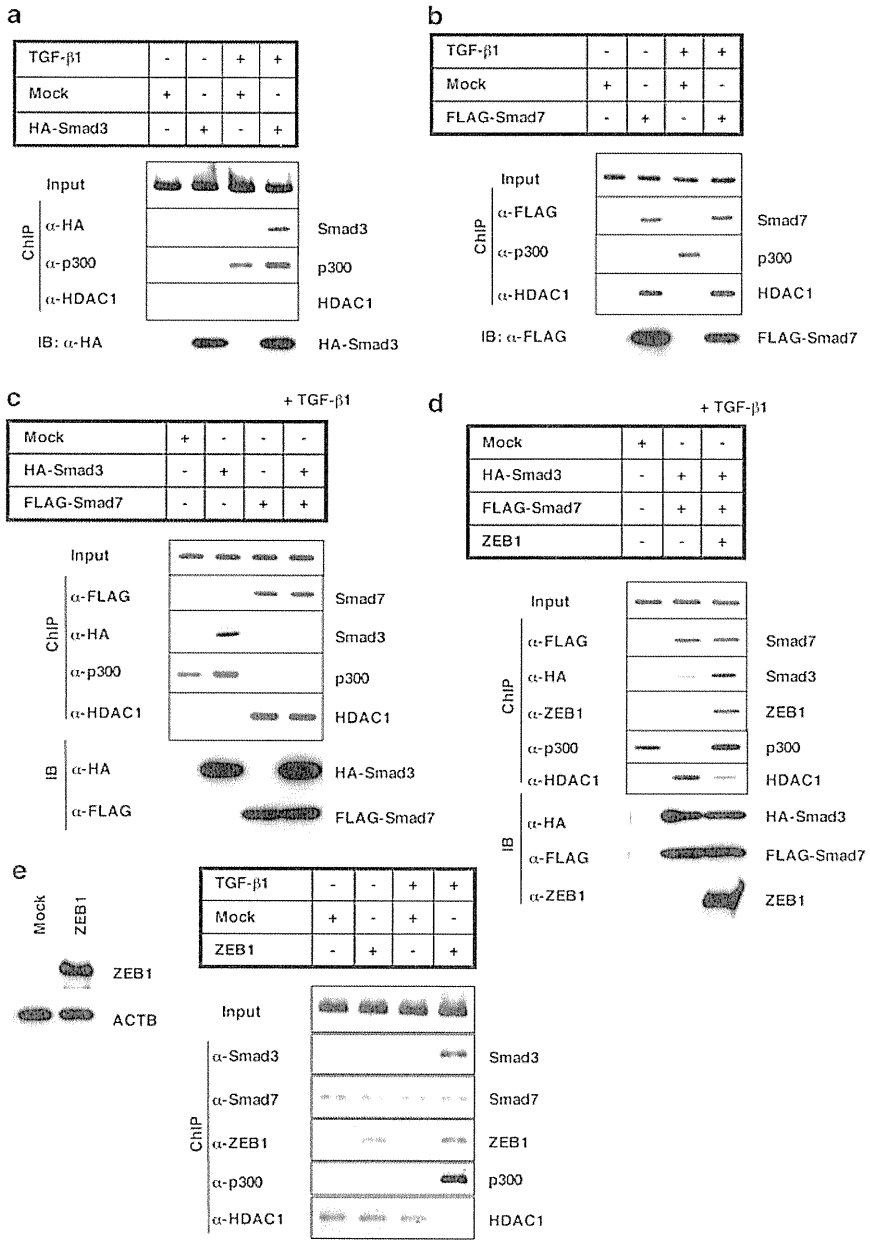

Figure 5 Smad7, ZEB1 and Smad3 are present in the transcription factor complex that binds to the Smad-responsive promoter. (**a**) Specific binding of Smad3 to the 3TP-Lux promoter upon TGF-β1 stimulation. After transfection with pcDNA3 (Mock) or HA-Smad3 and p3TP-Lux into HepG2 cells, the cells were treated with 5 ng/ml of TGF-β1 (+TGF-β1) or phosphate-buffered saline (PBS) (−TGF-β1) for 16 h. The cells were fixed with formaldehyde, sonicated and the chromatin fraction was immunoprecipitated using anti-HA, anti-p300 or anti-HDAC1 antibody. The precipitated DNA and 1% of the input cell lysates were amplified by PCR using specific primers for the 3TP-Lux promoter. As a control, the expression level of HA-tagged Smad3 protein was confirmed by western blot using an anti-HA antibody (IB). (**b**) Smad7 constantly binds to the 3TP-Lux promoter in either the presence or absence of TGF-β1. After transfection with pcDNA3 (Mock) or FLAG-Smad7 with p3TP-Lux and treatment with 5 ng/ml of TGF-β1 (+TGF-β1) or PBS (−TGF-β1) for 16 h, the HepG2 cells were chromatin immunoprecipitated (ChIP) by each indicated antibody. The precipitated DNAs were amplified by the 3TP promoter-specific primers. Smad7 protein expression was identified by an anti-FLAG antibody (IB). (**c**) Smad7 inhibits the DNA-binding of Smad3 and p300. HepG2 cells were transfected with p3TP-Lux and either empty vector (Mock) or plasmid vectors expressing HA-Smad3 and/or FLAG-Smad7 and treated with 5 ng/ml of TGF-β1 for 16 h. The cell lysates were subsequently subjected to ChIP with the indicated antibodies and precipitated DNAs were amplified using PCR for the 3TP promoter. A control western blot of the transfected cells is shown at the bottom (IB). (**d**) ZEB1 recruits the Smad3/p300 complex to the 3TP-Lux promoter. HepG2 cells were co-transfected with the expression vectors for HA-Smad3, FLAG-Smad7 and/or ZEB1, and p3TP-Lux plasmid and treated with 5 ng/ml of TGF-β1 for 16 h. The cell lysates were analyzed using ChIP. After immunoprecipitation with each indicated antibody, the 3TP promoter region was amplified by PCR using specific primers. A control western blot of the transfected cells is also shown. (**e**) Ectopic expression of ZEB1 causes efficient recruitment of the Smad3/p300 complex to the 3TP-Lux promoter in HTLV-1 (+) cell lines. MT2 cells were transfected with p3TP-Lux and either empty vector (Mock) or *ZEB1* expression vector and treated with 10 ng/ml of TGF-β1 for 24 h. The cell lysates were subjected to ChIP analysis with the indicated antibodies and primers specific for the 3TP promoter. A western blot of the transfected cells is shown in the left panel.

p3TP-Lux and *ZEB1* expression plasmids (Figure 5e). In the absence of TGF-β1, Smad7, ZEB1 and HDAC1 were detected on the 3TP promoter region; however, recruitment of Smad3 and p300 were detected along with a decrease of HDAC1 binding after TGF-β1 treatment. In Mock-transfected cells, protein complex of Smad7 and HDAC1 bound to the 3TP promoter region regardless of TGF-β1 treatment. To assess the possibility that ZEB1 might interfere with the interaction between Smad7 and HDAC1, we co-transfected GFP-Smad7 and FLAG-HDAC1 expression plasmids with increasing amounts of the *ZEB1* expression plasmid and subjected to co-immunoprecipitation using the anti-GFP antibody (Supplementary Figure 10). The HDAC1/Smad7 complex was clearly detected in the absence of ZEB1 transfection; however, the level of the HDAC1/Smad7 complex was decreased when increasing amounts of the *ZEB1* expression vector were transfected with both the GFP-Smad7 and FLAG-HDAC1 expression plasmids. These results suggest that ZEB1 recruits the Smad3/p300 complex to the 3TP promoter with the activation of TGF-β1 signal transduction despite the presence of Smad7 on the 3TP promoter region.

ZEB1 *expression extended the duration of* PAI-1 *and* p21 *transcriptional activation by TGF-β1 signaling in lymphoid cells*

The expression of I-Smads is quickly induced upon stimulation by TGF-β, and I-Smads may be part of the negative feedback control mechanism. We used semiquantitative RT–PCR to initially determine the expression pattern of ZEB1 and ZEB2, members of the zinc-finger E-box binding homeobox protein (ZFHX) family, in various hematopoietic cell populations. ZEB1 was expressed in the B- and T-cell populations in the spleen and the $CD4^+CD8^+$ DP, $CD4^+$ SP and $CD8^+$ SP T cells in the thymus (Figure 6a); however, ZEB2 was weakly expressed in the B-cell fraction in the spleen. Therefore, ZEB1 appears to have an important role in the late stages of T-cell development. To examine how *ZEB1* expression modulates TGF-β1 signaling, we used the murine interleukin-2 (IL-2)-dependent T-lymphoma cell line CTLL2, which has high expression of ZEB1 and low or no expression of Smad7, for this experiment. CTLL2 is known to be one of the T-cell lines that is highly responsive the treatment of TGF-β1, showing a decrease in cell viability to approximately 40%, compared to the control 2 days after TGF-β1 stimulation (Inge *et al.*, 1992; Hidaka *et al.*, 2008). To investigate the role that ZEB1 has in TGF-β1 signaling in CTLL2 cells, we transfected the cells with a ZEB1 shRNA vector (CTLL2-shZEB1) or a luciferase shRNA vector, which served as a control (CTLL2-shLuc), and examined the TGF-β1-induced transcription of *Smad6*, *Smad7*, *PAI-1* and *p21* by semiquantitative and quantitative RT–PCR. As previously reported, survival rates of CTLL2-shZEB1 cells increased to 60% after treatment with TGF-β1 (data not shown, Hidaka *et al.*, 2008). As shown in Figure 6b, treatment of TGF-β1 immediately induced *Smad6* and *Smad7* transcription as early as 30 min, and *PAI-1* mRNA was induced 1 h after TGF-β1 treatment. Peak expression of *PAI-1* mRNA in parental and CTLL2-shLuc cells continued for 12 h and then decreased to background levels 24 h after TGF-β1 treatment (Figure 6b). Similarly, in CTLL2-shZEB1 cells, *PAI-1* mRNA was induced 1 h after TGF-β1 treatment with a similar level of *PAI-1* mRNA as in control cells. However, the downregulation of *PAI-1* mRNA began as early as 4 h and continued to decrease to background levels at 12 h after TGF-β1 treatment (top, Figure 6c). Conversely, the expression of *p21* mRNA started to increase at 4 h after TGF-β1 treatment, whereas the peak was half that of control CTLL2 cells. Moreover, the highest expression level of *p21* lasted from 4 to 24 h in control cells; whereas that duration was shortened to 4–12 h in CTLL2-shZEB1 cells (bottom, Figure 6c). Thus, *ZEB1* expression in CTLL2 cells extended the duration of TGF-β1 signaling up to 24 h after TGF-β1 treatment. Because the duration of Smad3 phosphorylation in CTLL2-shZEB1 cells was not significantly different from those in the control cells (Supplementary Figure 11), it appears that *ZEB1* expression may enhance TGF-β1 signaling without affecting Smad3 phosphorylation in CTLL2 cells. To confirm the colocalization of ZEB1 and Smad7 in CTLL2 cells, we visualized both proteins by immunofluorescence, at the indicated times, after TGF-β1 treatment. ZEB1 constitutively localized to the nucleus, and Smad7, which was induced after TGF-β1 treatment, was also predominantly localized to the nucleus (Figure 6d). To confirm the protein complex of endogenous Smad3, Smad7 and ZEB1 on the TGF-β1 responsive promoter in CTLL2 cells after TGF-β1 treatment, we used ChIP using the corresponding specific antibody. Protein complex of Smad3, Smad7 and ZEB1 bound to the *p21* promoter in CTLL2 cells 12 h after TGF-β1 stimulation (top, Figure 6e). To confirm that Smad7 directly binds to the SRE in the *p21* promoter region, we constructed *p21* promoter reporter with mutated SRE for analyses of ChIP and the promoter activity induced by TGF-β1 (Seoane *et al.*, 2004). The mutated SRE in the *p21* promoter region totally abolished the DNA-binding activity of Smad7 by ChIP analysis (Figure 6f) and the level of the promoter activity was significantly reduced after TGF-β1 stimulation (Supplementary Figure 12), suggesting that Smad7 directly binds to the SRE with recruitment of the Smad3/ZEB1 complex. In MOLT4 cells, Smad7 and ZEB1 associated with the *p21* promoter regardless of TGF-β1 treatment and Smad3 recruitment could be detected upon stimulation with TGF-β1 (bottom, Figure 6e). Furthermore, knockdown of ZEB1 diminished the recruitment of Smad3 to the protein complex on the *p21* promoter in CTLL2 cells (Figure 6g), thus suggesting that ZEB1 was necessary for keeping Smad3 in the protein complex on the *p21* promoter with SRE to elongate the active status of TGF-β1 signaling. Figure 7a illustrates a model for the ZEB1-dependent transcriptional control in the TGF-β1 signaling pathway in CTLL2 cells. As a negative feedback mechanism, the expression of *Smad7* is induced within 1 h of TGF-β1

stimulation by Smad signal transduction pathways. The phosphorylated Smad3 cooperates with p300 and ZEB1 to activate many cellular genes within 1–12 h after TGF-β1 stimulation, including *PAI-1* and *p21*, through its ability to interact with several transcription factors, even though Smad7 protein accumulates in the cells at the later stages of development. When *ZEB1* expression was down-regulated by transfection with shZEB1, phosphorylated Smad3 could not bind to the *p21* promoter with SRE, which due to Smad7 interference, and *p21* transcription is shut off 4–12 h after TGF-β1 stimulation (Figure 7b). In the MOLT4 cell line, high expression of ZEB1 recruits phosphorylated Smad3 complex to the *p21* promoter region with the constitutive expression of Smad7, and weakly maintains TGF-β1 signaling with a survival rate of approximately 70% (Figure 7c). In HTLV-1 (+) cells, constitutive binding of Smad7 protein to the *p21* promoter region with SRE interferes with phosphorylated Smad3 complex to block TGF-β1 signaling, and most of the HTLV-1 (+) cells could survive after TGF-β1 treatment (Figure 7d).

Discussion

In this report, we showed that TGF-β signaling is enhanced by ZEB1, which binds to both R-Smads and I-Smads. Transcription of inhibitory I-Smad6 and I-Smad7 is immediately induced by the binding of

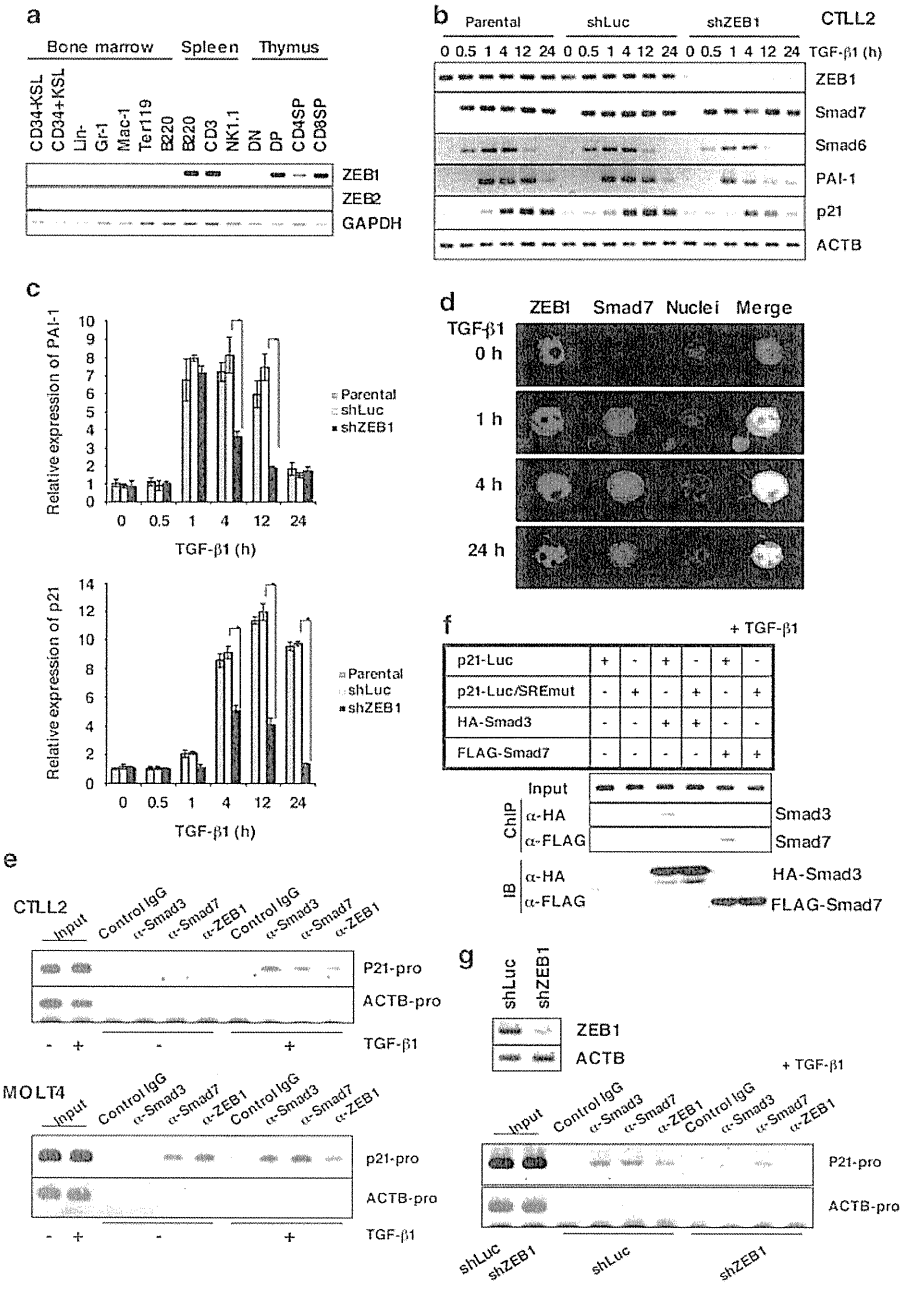

phosphorylated R-Smads to the promoter of Smad6 and Smad7 after TGF-β signaling. TGF-β signaling is suppressed by I-Smads in a negative feedback mechanism. In lymphoid cells, Smad7 is localized on the promoter with the SREs in the nucleus to suppress TGF-β signaling following induction of TGF-β; however, ZEB1 recruits the phosphorylated R-Smad complex to the promoter and enhances TGF-β signaling. Thus, ZEB1 may have important roles in the regulation of TGF-β1 signaling by binding to R-Smads and I-Smads. Moreover, while analyzing the molecular mechanism of resistance to TGF-β signaling in ATLL, we identified that both ZEB1 downregulation and Smad7 overexpression contribute to the TGF-β resistance.

Several reports have described the mechanism by which I-Smads inhibit TGF-β1 signaling. I-Smads located in the cytoplasm have been reported to bind TGF-β type I receptors, recruit E3 ubiquitin ligases (Smurfs) to type I receptors or bind to phosphorylated Smad1 and inhibit the formation of the R-Smad/Co-Smad complex (Hata *et al*., 1998; Souchelnytskyi *et al*., 1998; Kavsak *et al*., 2000; Ebisawa *et al*., 2001). Conversely, I-Smads

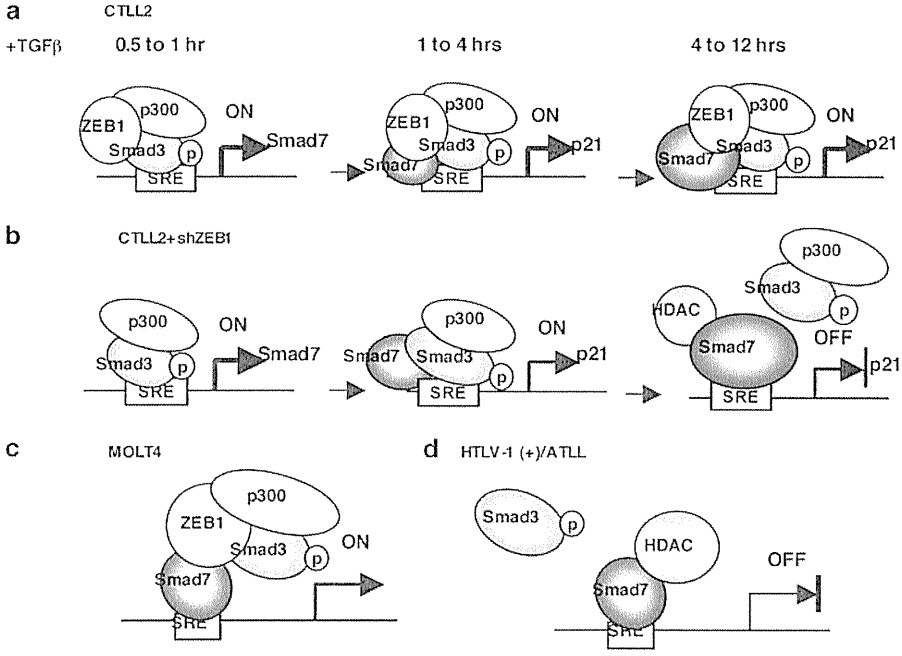

Figure 7 Schematic models for Smad-dependent transcriptional repression and transcriptional activation complexes on SRE in various kinds of cell lines. (**a**) CTLL2; (**b**) CTLL2 transfected with shZEB1; (**c**) MOLT4, T-ALL cell line and (**d**) HTLV-1 (+)/ATLL cells. See text for details.

Figure 6 ZEB1 regulates the duration of Smad-dependent transcription. (**a**) Semiquantitative RT–PCR analysis of *ZEB1* and *ZEB2* mRNA expression was performed with mRNA isolated from $CD34^-$ KSL cells, $CD34^+$ KSL cells, lineage marker$^-$ cells, $Gr\text{-}1^+$ neutrophils, $Mac\text{-}1^+$ monocytes/macrophages, $TER119^+$ erythroblasts and $B220^+$ B lymphoid cells from the bone marrow, $B220^+$ B lymphoid cells, $CD3^+$ T lymphoid cells and $NK\text{-}1.1^+$ natural killer cells from the spleen. In addition, mRNA was isolated from $CD4^-CD8^-$, $CD4^+CD8^+$, $CD4^+CD8^-$ and $CD4^-CD8^+$ T-lymphoid cells from the thymus of adult mice. The expression of glyceraldehyde-3-phosphate dehydrogenase (*GAPDH*) is shown at the bottom as a control. (**b**) CTLL2 cells were untransfected (Parental) or transfected with the control luciferase-specific shRNA vector (shLuc), or the ZEB1-specific shRNA vector (shZEB1) and then treated with 10 ng/ml of TGF-β1. Total RNA was isolated at the indicated time points and semiquantitative RT–PCR was performed with specific primers for *ZEB1*, *Smad6*, *Smad7*, *PAI-1*, *p21* and β-actin. (**c**) Quantitative real-time PCR analysis of *PAI-1* (top) and *p21* (bottom) mRNA expression in the same conditioned CTLL2 cell lines as **b**. Student's *t*-test was used for the statistical analysis, and $P<0.05$ (asterisk) was considered significant. (**d**) Subcellular localization of ZEB1 and Smad7 in the CTLL2 cell lines at the indicated time periods after treatment with 10 ng/ml of TGF-β1. The localization of endogenous ZEB1 and Smad7 was detected by indirect immunofluorescence using an anti-ZEB1 (green, Alexa Fluor 488) and anti-Smad7 antibody (red, Alexa Fluor 555) using the same strategy as described in Figure 3. The cells were analyzed by confocal microscopy, and a DAPI (4,6-diamidino-2-phenylindole) stain was used to visualize the position of the nuclei (blue). (**e**) Protein complex of Smad3, Smad7 and ZEB1 bound to the *p21* promoter after TGF-β1 treatment. Chromatin from CTLL2 (top) and MOLT4 (bottom) cells treated with or without 10 ng/ml of TGF-β1 for 12 h was immunoprecipitated with antibodies against Smad3, Smad7, ZEB1 or normal rabbit serum (as negative controls) and immunoprecipitated DNA was analyzed by PCR using the indicated primer pairs. PCR using primers specific for the β-actin (*ACTB*) promoter was included for the specificity of the ChIP assay. (**f**) CTLL2 cells were co-transfected with a p21-Luc or p21-Luc/SREmut reporter construct and/or expression vectors for either HA-Smad3 or FLAG-Smad7 and treated with 10 ng/ml of TGF-β1 for 12 h. The cell lysates were analyzed using ChIP. A control western blot of the transfected cells is also shown. (**g**) Occupancy of Smad3 is reduced in the protein complex on the *p21* promoter with SRE in CTLL2-shZEB1 cells. CTLL2 cells were transfected with the control shRNA vector (shLuc), or the ZEB1-specific shRNA vector (shZEB1) and treated with 10 ng/ml of TGF-β1 for 12 h. The cell lysates were analyzed using ChIP. Semiquantitative RT–PCR for *ZEB1* and β-actin mRNA are shown at the top panel.

that reside in the nucleus interact with the transcriptional co-repressors Hoxc-8 or CtBP to inhibit BMP-induced transcription or bind to DNA to competitively inhibit the formation of the Smad/DNA complex (Bai *et al.*, 2000; Lin *et al.*, 2003; Zhang *et al.*, 2007). In ATLL cells, Smad7 predominantly localizes to the nucleus and binds to the promoter region of TGF-β1 responsive genes with SRE to inhibit formation of the R-Smad/DNA complex. The differential localization of Smad7 between cell types is currently unknown; however, Smurf-mediated nuclear export of Smad7 has been shown in several studies (Kavsak *et al.*, 2000; Suzuki *et al.*, 2002). In our study using DNA microarrays, we found that the expression level of Smurf1 in acute-type ATLL cells was higher than in $CD4^+$ T lymphocytes from normal volunteers; however, the expression of Smurf2 was lower in ATLL cells (data not shown). Therefore, further studies are needed to clarify the mechanism of Smad7 nuclear localization in ATLL cells.

I-Smads have important roles in the negative feedback mechanism of Smad signaling, and protein phosphatase 1A was recently identified as a Smad phosphatase that terminates TGF-β1 signaling (Lin *et al.*, 2006). Protein phosphatase 1A enhances the disassembly of the activated Smad complex by dephosphorylation of TGF-β1-activated Smad2/3 and promotes nuclear export of dephosphorylated Smad2/3. In T lymphocytes, transcriptional activation by TGF-β1 signaling was terminated within 24 h in both the control CTLL2 and CTLL2-shZEB1 cells, suggesting that protein phosphatase 1A terminates TGF-β1 signaling within 24 h. However, expression of ZEB1 in CTLL2 cells elongated the duration of TGF-β1-induced transcriptional activation of *PAI-1* and *p21* to overcome the suppressor activity of I-Smad6 and I-Smad7 until 24 h. Therefore, we speculate that the elongation of TGF-β1 signaling by ZEB1 is necessary for suppression of the cell growth of T lymphocytes during T-cell differentiation by TGF-β1.

In this study, we showed that ZEB1 interacts with both R-Smads and I-Smads to enhance TGF-β1 signaling and counteracts the Smad7-mediated inhibition of TGF-β1 signaling. We showed that ZEB1 is specifically expressed in $CD4^+CD8^+$ DP lymphocytes through $CD4^+$ SP T lymphocytes (Figure 6a), and *ZEB-1*-deficient mice frequently develop $CD4^+$ T-lymphoma/leukemia (Hidaka *et al.*, 2008). This suggests that the expression of ZEB1 during the late stages of T-cell differentiation is necessary for enhancing the growth-inhibitory effect of TGF-β1 on $CD4^+$ T cells. In addition, recent studies have shown that in Sézary syndrome, an aggressive cutaneous T-cell lymphoma/leukemia, genomic deletion of *ZEB1* has been detected in approximately half of patients (Vermeer *et al.*, 2008). Although Smad7 overexpression has not yet been reported in Sézary syndrome, downregulation of ZEB1, in combination with Smad7 overexpression, may be an important event for the development of peripheral types of T-cell leukemia/lymphoma.

Materials and methods

Cell lines

MOLT4, MKB1, KAWAI and Jurkat are HTLV-1-negative human T-ALL cell lines (Schneider *et al.*, 1977). MT2 and Hut102 are HTLV-1-infected T-cell lines with polyclonal viral integration (Miyoshi *et al.*, 1981). KOB, SO4 and KK1 are IL-2-dependent ATLL cell lines (Yamada *et al.*, 1996). ED and S1T are IL-2-independent ATLL cell lines (Okada *et al.*, 1985). In this report, both the HTLV-1-infected cell lines and ATLL-derived cell lines were referred to as HTLV-1-positive cell lines. CTLL2 is an IL-2-dependent murine cytotoxic T-cell line (Gillis and Smith, 1977). These cell lines were maintained in RPMI 1640 medium (Invitrogen, Carlsbad, CA, USA) supplemented with 10% fetal calf serum (FCS), either with or without IL-2. HEK293T (human embryonic kidney) and HepG2 (human hepatocellular carcinoma) cells were cultured in Dulbecco's modified Eagle's medium (Invitrogen) with 10% fetal calf serum.

Conflict of interest

The authors declare no conflict of interest.

Acknowledgements

This work was supported by Grants-in-Aid for Scientific Research of Priority Area from the Ministry of Education, Culture, Sports, Science and Technology, Japan; Leukemia Research fund; Research fund from Miyazaki Prefecture Collaboration of Regional Entities for the Advancement of Technological Excellence, JST (KM) and Young Scientists (B) (19790344) of Japan Society for the Promotion of Science (SN).

References

Arnulf B, Villemain A, Nicot C, Mordelet E, Charneau P, Kersual J *et al.* (2002). Human T-cell lymphotropic virus oncoprotein Tax represses TGF-beta 1 signaling in human T cells via c-Jun activation: a potential mechanism of HTLV-I leukemogenesis. *Blood* **100**: 4129–4138.

Bai S, Shi X, Yang X, Cao X. (2000). Smad6 as a transcriptional corepressor. *J Biol Chem* **275**: 8267–8270.

Blobe GC, Schiemann WP, Lodish HF. (2000). Role of transforming growth factor β in human disease. *N Engl J Med* **342**: 1350–1358.

Derynck R, Akhurst RJ, Balmain A. (2001). TGF-beta signaling in tumor suppression and cancer progression. *Nat Genet* **29**: 117–129.

Ebisawa T, Fukuchi M, Murakami G, Chiba T, Tanaka K, Imamura T *et al.* (2001). Smurf1 interacts with transforming growth factor-beta type I receptor through Smad7 and induces receptor degradation. *J Biol Chem* **276**: 12477–12480.

Gillis S, Smith KA. (1977). Long term culture of tumour-specific cytotoxic T cells. *Nature* **268**: 154–156.

Hata A, Lagna G, Massagué J, Hemmati-Brivanlou A. (1998). Smad6 inhibits BMP/Smad1 signaling by specifically competing with the Smad4 tumor suppressor. *Genes Dev* **12**: 186–197.

Hidaka T, Nakahata S, Hatakeyama K, Hamasaki M, Yamashita K, Kohno T *et al.* (2008). Down-regulation of TCF8 is involved in the

leukemogenesis of adult-T cell leukemia/lymphoma. *Blood* **112**: 383–393.

Inge TH, McCoy KM, Susskind BM, Barrett SK, Zhao G, Bear HD. (1992). Immunomodulatory effects of transforming growth factor-beta on T lymphocytes. Induction of CD8 expression in the CTLL-2 cell line and in normal thymocytes. *J Immunol* **148**: 3847–3856.

Kavsak P, Rasmussen RK, Causing CG, Bonni S, Zhu H, Thomsen GH *et al.* (2000). Smad7 binds to Smurf2 to form an E3 ubiquitin ligase that targets the TGF beta receptor for degradation. *Mol Cell* **6**: 1365–1375.

Kim SJ, Kehrl JH, Burton J, Tendler CL, Jeang KT, Danielpour D *et al.* (1990). Transactivation of the transforming growth factor beta 1 (TGF-beta 1) gene by human T lymphotropic virus type 1 tax: a potential mechanism for the increased production of TGF-beta 1 in adult T cell leukemia. *J Exp Med* **172**: 121–129.

Kingsley DM. (1994). The TGF-beta superfamily: new members, new receptors, and new genetic tests of function in different organisms. *Genes Dev* **8**: 133–146.

Lin X, Duan X, Liang YY, Su Y, Wrighton KH, Long J *et al.* (2006). PPM1A functions as a Smad phosphatase to terminate TGFbeta signaling. *Cell* **125**: 915–928.

Lin X, Liang YY, Sun B, Liang M, Shi Y, Brunicardi FC *et al.* (2003). Smad6 recruits transcription corepressor CtBP to repress bone morphogenetic protein-induced transcription. *Mol Cell Biol* **23**: 9081–9093.

Miyoshi I, Kubonishi I, Yoshimoto S, Akagi T, Ohtsuki Y, Shiraishi Y *et al.* (1981). Type C virus particles in a cord T-cell line derived by co-cultivating normal human cord leukocytes and human leukaemic T cells. *Nature* **294**: 770–771.

Mochizuki N, Shimizu S, Nagasawa T, Tanaka H, Taniwaki M, Yokota J *et al.* (2000). A novel gene, MEL1, mapped to 1p36.3 is highly homologous to the MDS1/EVI1 gene and is transcriptionally activated in t(1;3)(p36;q21)-positive leukemia cells. *Blood* **96**: 3209–3214.

Mori N, Morishita M, Tsukazaki T, Giam CZ, Kumatori A, Tanaka Y *et al.* (2001). Human T-cell leukemia virus type I oncoprotein Tax represses Smad-dependent transforming growth factor beta signaling through interaction with CREB-binding protein/p300. *Blood* **97**: 2137–2144.

Okada M, Maeda M, Tagaya Y, Taniguchi Y, Teshigawara K, Yoshiki T *et al.* (1985). TCGF (IL 2)-receptor induction Factor (S). II. Possible role of ATL-derived factor (ADF) on constitutive IL 2 receptor expression of HTLV-1(+) T cell lines. *J Immunol* **135**: 3995–4003.

Postigo AA. (2003). Opposing functions of ZEB proteins in the regulation of the TGFbeta/BMP signaling pathway. *EMBO J* **22**: 2443–2452.

Schneider U, Schwenk HU, Bornkamm G. (1977). Characterization of EBV-genome negative 'null' and 'T' cell lines derived from children with acute lymphoblastic leukemia and leukemic transformed non-Hodgkin lymphoma. *Int J Cancer* **19**: 621–626.

Shi Y, Massagué J. (2003). Mechanisms of TGF-beta signaling from cell membrane to the nucleus. *Cell* **113**: 685–700.

Seoane J, Le HV, Shen L, Anderson SA, Massagué J. (2004). Integration of Smad and forkhead pathways in the control of neuroepithelial and glioblastoma cell proliferation. *Cell* **117**: 211–223.

Souchelnytskyi S, Nakayama T, Nakao A, Morén A, Heldin CH, Christian JL *et al.* (1998). Physical and functional interaction of murine and Xenopus Smad7 with bone morphogenetic protein receptors and transforming growth factor-beta receptors. *J Biol Chem* **273**: 25364–25370.

Suzuki C, Murakami G, Fukuchi M, Shimanuki T, Shikauchi Y, Imamura T *et al.* (2002). Smurf1 regulates the inhibitory activity of Smad7 by targeting Smad7 to the plasma membrane. *J Biol Chem* **277**: 39919–39925.

Tsukasaki K, Krebs J, Nagai K, Tomonaga M, Koeffler HP, Bartram CR *et al.* (2001). Comparative genomic hybridization analysis in adult T-cell leukemia/lymphoma: correlation with clinical course. *Blood* **97**: 3875–3881.

van Grunsven LA, Schellens A, Huylebroeck D, Verschueren K. (2001). SIP1 (Smad interacting protein 1) and deltaEF1 (delta-crystallin enhancer binding factor) are structurally similar transcriptional repressors. *J Bone Joint Surg Am* **83-A**: Suppl 1 (Part 1): S40–S47.

Vermeer MH, van Doorn R, Dijkman R, Mao X, Whittaker S, van Voorst Vader PC *et al.* (2008). Novel and highly recurrent chromosomal alterations in Sézary syndrome. *Cancer Res* **68**: 2689–2698.

Yamada Y, Ohmoto Y, Hata T, Yamamura M, Murata K, Tsukasaki K *et al.* (1996). Features of the cytokines secreted by adult T cell leukemia (ATL) cells. *Leuk Lymphoma* **21**: 443–447.

Yasunaga J, Matsuoka M. (2003). Leukemogenesis of adult T-cell leukemia. *Int J Hematol* **78**: 312–320.

Yoshida M, Nosaka K, Yasunaga J, Nishikata I, Morishita K, Matsuoka M. (2004). Aberrant expression of the MEL1S gene identified in association with hypomethylation in adult T-cell leukemia cells. *Blood* **103**: 2753–2760.

Zhang S, Fei T, Zhang L, Zhang R, Chen F, Ning Y *et al.* (2007). Smad7 antagonizes transforming growth factor beta signaling in the nucleus by interfering with functional Smad-DNA complex formation. *Mol Cell Biol* **27**: 4488–4499.

Supplementary Information accompanies the paper on the Oncogene website (http://www.nature.com/onc)